High Data-Rate Packet Communications for Cellular Networks Using CDMA: Algorithms and Performance

Sarath Kumar and Sanjiv Nanda, *Member, IEEE*

Abstract— The advantages of code division multiple access (CDMA) for cellular voice have become well known, and IS-95-based systems have now been widely deployed. Attention is now focused on higher data-rate packet services for cellular systems. Although many packet multiple access schemes have been studied over the years, researchers have often studied single cell performance and ignored reuse. Moreover, direct sequence spread spectrum (DSSS) has been considered unsuitable for high data-rate packet multiple access since spreading limits the permitted data rates, DSSS requires large overhead (preambles) for acquisition and requires closed-loop power control.

In this paper, we describe a scheme for high data-rate packet service using CDMA that addresses all of the above problems and has been standardized in Revision B of IS-95. A low rate fundamental code channel is maintained that eliminates the need for long preamble and provides closed-loop power control. Reuse is managed by the infrastructure through a "burst-level" admission control based on load and interference-level measurements at the base stations and mobiles.

We report on the feasibility of such a burst-mode packet data service for cellular CDMA networks. The focus is not only on the performance of high data-rate users, but also on the impact on voice users sharing the CDMA band. We propose a multitiered performance analysis methodology consisting of a mix of static simulations, dynamic simulations at different time scales, and analytic methods to address the various feasibility issues: impact on coverage; capacity; power control; and effectiveness of burst admission algorithms. We expect that detailed performance work on all aspects discussed in this paper will continue in the future. However, based on the current study, we can conclude that the proposed approach is well suited for third-generation wideband CDMA systems being considered for standardization throughout the world.

Index Terms—Burst admission, CDMA packet data, high data-rate services, load and interference-based dynamic assignment (LIDA), wireless data.

I. INTRODUCTION

FUTURE wide-area (cellular) wireless networks will support a variety of services. Users with very different application- and location-specific, time-varying rate and quality of service (QOS) requirements will have to be accommodated. A mobile terminal may set up and modify sessions for voice, data, image, as well as video through wireless connections to the base station (BS). In order to provide such services, the network must be able to statistically multiplex users with different rates and/or QOS requirements while maximizing the spectral efficiency. Moreover, the network should provide fair capacity sharing among all busy users and allow peak capacity access by one user if all others are idle. Thus, the attraction of packet-based wireless networks is evident. A technology that meets the above requirements and can evolve from emerging digital cellular systems will be quite attractive as a basis for personal communication services (PCS).

In recent years, much research has focused on high-speed packet wireless access. Wireless ATM standardization is currently in progress [1], [2]. Some diverse samples of work on packet multiple access for wireless networks include PRMA [3], WaveLAN [4], and DQRUMA [5]. Although attempts have been made to address cellular-type reuse for such medium access control procedures (MAC's), most work on MAC's has ignored reuse issues. An exception is the work by Whitehead [6] to extend the WaveLAN protocols for efficient access with reuse. Also, dynamic packet-by-packet cellular reuse in a time division multiple access (TDMA) system is studied in [7].

The advantages of code division multiple access (CDMA) [8], [9] for cellular voice have become well known. In contrast to orthogonal systems such as TDMA or frequency division multiple access (FDMA), frequency planning or "orthogonality" coordination (channel allocation) between cells and within the same cell are greatly simplified. The reason is that, unlike TDMA and FDMA where the reuse constraints usually account for the worst case (e.g., ninety-fifth percentile) interferer, reuse in CDMA is based on the average interference seen from a large number of low-power users. Due to this interference averaging property, CDMA simply translates voice activity factor and antenna sectorization into capacity gains. Furthermore, RAKE receivers resolve the multipath components of the spread spectrum signal and translate it into diversity gain.

On the other hand, spread spectrum has not been pursued as a viable method of providing higher data rates and packet multiple access over wireless. This is primarily due to the following reasons.

1) Spreading limits the permissible data rates in the limited wireless spectrum.
2) Signal acquisition for packet access using spread spectrum requires large overhead and delay.

3) Dynamic slotted time-division access can be more efficient compared to CDMA [10].

In this paper we address these problems in providing higher data-rate packet mode service using CDMA. When supporting higher data rates in a system with mixed traffic, the challenge is to design an access control mechanism which allows one or more users to get high data-rate bursts without impacting the QOS to the voice users. The focus of this paper is on the design and performance evaluation of such an access control mechanism. The issues discussed above are addressed as follows.

1) Acquisition delays and overhead are minimized through the use of a low overhead acquisition and tracking (fundamental) code channel even when idle. The fundamental code channel also acts as a dedicated signaling channel for burst control and signaling.

2) The scheme permits a single user to access the entire bandwidth by limiting the spreading. Different data rates and QOS for diverse user classes are managed through variable spreading gain and coding. For the duration of the higher data-rate transmission, in addition to the fundamental code channel, the mobile is assigned supplemental code channel(s).

3) Efficient use of the spectrum with diverse user classes is handled in a distributed manner through the management of aggregate interference (over time). This problem has greatly reduced dimensionality compared to dynamic slotted time division access, which requires resource management in the time, frequency, and reuse dimensions.

A. Design Approach: Load and Interference-Based Demand Assignment (LIDA) [15], [16]

We focus on packet data services over interference-limited cellular wireless systems. We assume that the forward (BS to mobile) and reverse (mobile to BS) links are on different frequency bands as is the case with virtually all cellular systems today.

The CDMA packet access schemes considered in this paper are asymmetric, that is, the instantaneous bandwidth requirement for the forward and reverse links can be unequal. Burst allocation on either the forward or the reverse link is handled by examining power and interference constraints and through the use of interference measurements and path loss information gathered from the distributed mobiles and neighbor BS's.

Simplified schemes that limit the amount of communication required for burst allocation are also described. For example, on the forward link the interference constraint can be translated into a transmit power constraint and the network can implement a centralized scheduled power allocation to multiple users that guarantees efficient bandwidth utilization. Bandwidth coordination between distributed users is more challenging on the multiple access reverse link. We have designed distributed burst allocation schemes for both the forward and reverse links.

Consider a system in which distributed high data-rate users in a cellular environment share the cellular CDMA band with conventional mobile cellular voice and circuit-mode data users. To control the interference variation in cellular CDMA systems serving mixed traffic, we design a network control that accounts for channel loading and interference. It dynamically assigns higher data rates to requesting users while simultaneously adjusting the QOS for each user according to service requirements. Higher data rates are assigned to users on either the forward or the reverse channel, independently, by permitting users to transmit on multiple code channels simultaneously or by reducing the spreading. QOS is adjusted by changing the coding rate or through power control with a target frame error rate (FER) or target E_b/N_o on the channel. The network uses a control strategy that accounts for channel loading, interference, and soft handoff in making rate assignment and QOS decisions. It ensures priority for voice users or circuit-mode data users, if so desired. Thus, dynamic, packet-like demand-assigned access enables users with different services to access the channel at desired rates and QOS requirements. With best-effort-type QOS guarantees, the high data-rate service is well suited for typical internet and web applications [including services based on cellular digital packet data (CDPD) and mobile IP].

Based on computation of the in-cell and out-of-cell interference caused by a high-rate data user, LIDA algorithms have been designed to allow burst access at rates up to M times the full rate, based on the following:

1) the load information in the cell and its neighbors;
2) the pilot strength measurements provided by the mobile;
3) coordination of the burst rate, burst length, and burst starting time between neighbor cells.

B. Focus of this Paper

This paper reports on the extensive protocol design and performance analysis work done to study high data-rate packet services. We begin with a static capacity analysis for the reverse link, based on the computation of interference constraints at a cell and its neighbors (Section II). We use this as motivation for proposing a burst-mode packet access scheme in which high data rates are assigned to mobiles for short burst durations, based on load and interference measurements. The solution proposed using the approach is described in Section III. A number of features that permit efficient assignment of resources are also discussed. Optimal resource allocation algorithms can be written using the following information (Section IV).

1) Pilot strength information reported by the mobile: used to estimate path loss for the reverse link and the E_b/N_0 on the forward link.
2) Forward and reverse link load at each cell and its neighbors.

These schemes are studied using a combination of static and dynamic simulations. The performance analysis methodology that we follow is described in Section V. Monte Carlo simulation and analysis is used to study "static" coverage and capacity. However, achievable performance depends on the dynamics of mobility, pilot strength measurements, soft handoffs, and message-processing delays in the system. The dynamics determine the burst admission probability, burst length, and

performance during bursts. In Section V-B–V-C we describe our hybrid simulation and analysis approach for performance analysis that addresses the dynamics of the problem.

Forward and reverse link coverage and capacity are affected differently by users with higher data rates. On the forward link, a small fraction of the users are assigned a large fraction of the transmit power budget. Hence, coverage and capacity are limited if the higher data-rate user is closer to the boundary. This analysis is presented in Section VI. Soft handoff provides seamless service and significant performance gains for voice– and circuit-mode services. But for packet-mode services that involve high-rate data burst transmission for short durations, it may be beneficial to transmit supplemental channels on the forward link from only a subset of the soft handoff legs. While there is performance degradation without soft handoff, acceptable performance may be achieved for low- to medium-speed mobiles, especially when the burst durations are short. The tradeoffs between the performance degradation and the overall system capacity gains are quantified in Section VI-C.

On the reverse link, the higher data-rate user in soft handoff uses up capacity in multiple cells. Reverse link capacity results and burst performance are discussed in Section VII. The mobile's power budget may further limit reverse link coverage. We discuss this issue in Section VII-C. CDMA systems rely on a tight reverse link power control. Each mobile runs its own independent power control to combat the path loss variations and the aggregate interference. With higher data-rate operation, the statistics of aggregate interference are different. We discuss the impact on reverse link performance and capacity in Section VIII.

We conclude that the proposed burst-mode packet data service is viable for CDMA cellular systems (Section IX). As the international third-generation cellular standards converge toward wideband CDMA, our approach and results can be applied to those systems.

C. Standards Activity

New messages and procedures have been standardized in Revision B of the IS-95 CDMA cellular standard [22] that accommodate such burst-mode operation. The procedures are general, and we expect that several emerging third-generation cellular technologies based on CDMA will incorporate these schemes as well. We believe these interference-management methods are quite powerful and may provide the best engineering solution to providing high data-rate access in an interference constrained outdoor cellular environment. In particular, the developing U.S. third-generation CDMA standard provides for a similar access method, where higher data rates on the forward link are handled through a combination of variable Walsh spreading and multiple code channels, while on the reverse link, higher data rates are handled through variable spreading gain. We refer the reader to [11] for a high-level presentation of these proposals and a comparison of IS-95 Rev B and cdma2000.

II. MOTIVATION FOR BURST-MODE APPROACH

We first extend the CDMA reverse link interference calculations to the case when there is a single high data-rate user multiplexed with voice users. We find that adjacent-cell interference is critical in determining permitted data rate.

A. Cellular Interference Calculations

In a voice-only CDMA cellular system, each in-cell interferer causes identical interference at the BS, while the average out-of-cell interferer aggregated from all cells in a regular hexagonal grid cellular system appears to be equivalent to η in-cell users. Assuming a path loss exponent of $\delta = 4, \eta$ has been computed to be around 0.55 [8]. In a system with N_{nom} voice users per cell, the total nominal interference at each BS is

$$I_0 = aN_{\text{nom}}(1 + \eta) \tag{1}$$

where a is the speech activity factor. We will use I_0 as the reference load in the subsequent discussion.

Now let us assume there is one active high data-rate user in the host cell transmitting at M times full rate of the voice user. The total interference in the host cell and in the closest neighboring cell is computed as $M\eta_d(r)$, where r is the distance from the active high data-rate mobile to its host cell site. $\eta_d(r) = 1$ for the host cell since it is power controlled by that cell and $\eta_d(r) \approx r^4/(2R - r)^4$ for the neighboring cell, where R is the cell radius. The access control mechanism for high data-rate users must satisfy the constraint

$$I_d(r) \leq I_0 \tag{2}$$

in all the cells, where $I_d(r)$ is the total interference with the data user in the system.

In the presence of shadow fading, the average interference at the cell site for the basic voice-only system is modified as in [8]. Let us denote it as $I_0^{(s)} = aN_{\text{nom}}(1 + \eta^{(s)})$, where superscript s indicates the presence of shadow fading. Similarly, in an integrated voice and data system, the interference factor for a data user in a neighboring cell is $\eta_d^{(s)}(z_1, z_2) = z_1/z_2$, where z_1 and z_2 are the path loss (radio distance) of the mobile to the host cell and to the neighboring cell, respectively. Practically, the ratio z_1/z_2 for the reverse link may be approximated by the ratio of time-averaged (forward link) pilot strength measurements from the two cells.

B. Capacity Calculations with High Data-Rate User

To quantify our discussion above, we consider three-sectored cells and focus on the out-of-cell interference contribution from the two dominant neighboring cells. Let us consider the interference seen at sector γ of cell I in Fig. 15. Let i_α, i_β and i_γ denote the average reverse link interference at cell I, sector γ, generated by a user in sectors α, β, and γ, respectively, of cell II. Let i_0 denote the average interference at cell I, sector γ, due to cell II, when there is one user per sector in cell II. Then we have $i_0 = i_\alpha + i_\beta + i_\gamma$. These interference factors are computed in the Appendix. Note that because of symmetry, the interference factor from cell III is also the same. Since the total external interference at cell I, sector γ is lower bounded by the interference coming from cells II and III, we have $\eta > 2i_0$.
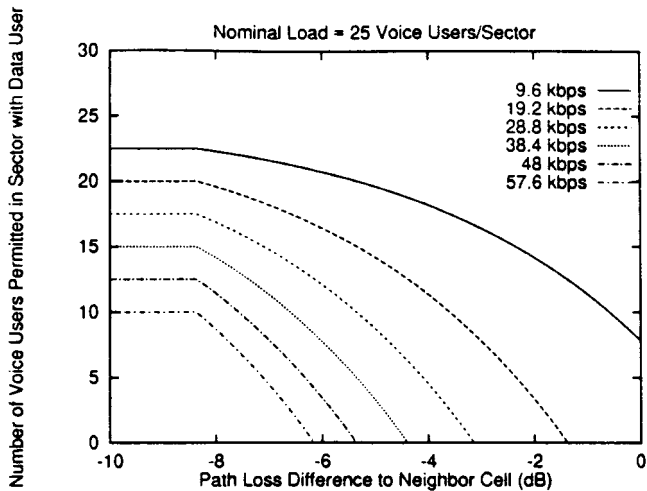
Fig. 1. Number of voice users permitted in the sector with high data-rate user with nominal load in other sectors.
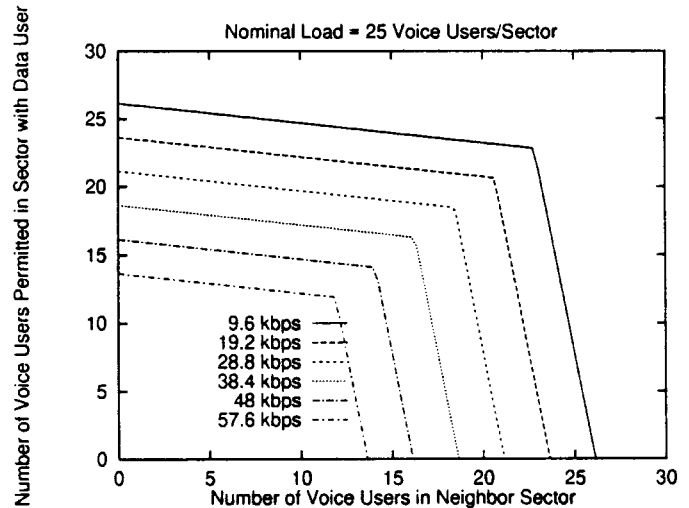

Fig. 2. Number of voice users permitted in sector with high data-rate user and neighbor sector. The high data-rate user has equal path loss to both cells and transmits at rate 9.6 kb/s, ..., 57.6 kb/s.
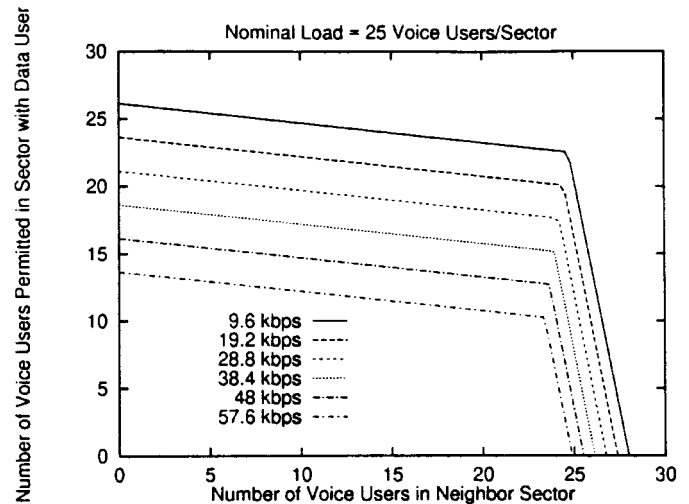

Fig. 3. Number of voice users permitted in sector with high data-rate user and neighbor sector. The high data-rate user has 6 dB higher path loss to neighbor cell and transmits at rate 9.6 kb/s, ..., 57.6 kb/s.

Using the per-sector interference factors from column two (column three) of Table XI, we obtain the corresponding value of i_0 with (without) shadow fading. A shadow fading standard deviation of 6.8 dB is used in the example tradeoffs below.

Assume a nominal load in the system of $N_{\mathrm{nom}} = 25$ voice users per sector[1] in all sectors except the host sector α of cell II. In the host sector, assume there are N_v voice users and one active (transmitting) high-rate data user at M times the basic data rate. The basic data rate is assumed to be the same as the full rate for voice (9.6 kb/s for IS-95 Rate Set 1). Below, we study the tradeoff between N_v and M. Access control is used to pick the single data user that is active and transmitting on the shared high data-rate packet channel at any instant. Consider the case with shadow fading. The total interference in the host sector can be expressed as follows:

$$I_{\mathrm{II},\alpha} = a(N_v + 2N_{\mathrm{nom}}i_0) + M. \tag{3}$$

In the handoff sector (the closest neighboring sector with respect to that data user, i.e., sector γ of cell I), the total interference is

$$I_{\mathrm{I},\gamma}(z_1, z_2) = aN_{\mathrm{nom}}(1 + i_0 + i_\beta + i_\gamma)$$
$$+ aN_v i_\alpha + M\eta_d^{(s)}(z_1, z_2). \tag{4}$$

Using $I_{\mathrm{I},\alpha}, I_{\mathrm{II},\gamma} < I_0 = aN_{\mathrm{nom}}(1 + 2i_0)$ with (3) and (4), we obtain two bounds on the maximum number of voice users with which the data users will be allowed to transmit at M times the basic rate

$$N_v \leq N_{\mathrm{nom}} - M/a \tag{5}$$
$$N_v \leq N_{\mathrm{nom}} - M/(ai_\alpha)(z_1/z_2). \tag{6}$$

Fig. 1 shows N_v as a function of the ratio z_1/z_2 (dB) of path losses. N_v represents the maximum number of voice users in the sector when the data user is allowed to transmit the burst at M ($M = 1, \ldots, 6$) times the basic data rate of 9.6 kb/s. The burst request at M times the basic rate cannot be allowed

[1] This number is chosen for illustration purposes. The actual voice CDMA voice capacity is a function of several system and environment parameters.

if the number of voice users exceeds N_v. Here we have used a speech activity factor $a = 0.4$.

In Fig. 1, the flat part corresponds to the region where the in-cell interference dominates. Here the permitted data rate depends on the current bandwidth used by voice users. The drop in the curves corresponds to the region where adjacent cell interference dominates. We have assumed that there are N_{nom} voice users at all neighbor sectors. By trading off voice users in the neighbor cells higher data rates can be carried, as discussed next. Figs. 2 and 3 show this tradeoff.

A high data-rate user in a position to cause large interference at a neighbor cell is permitted to transmit at the high rate only if the number of voice users is small in the cell and its neighbors. On the other hand, if the high-rate user is in a position that causes little interference to neighbor cells, then the number of voice users in the neighbor cell has very little effect on whether the user can be permitted to transmit at a high rate. To illustrate this tradeoff consider a particular situation where

Mobile Station   **BS/MSC**

Call Origination: Packet Data Service Option

Service Negotiation:
Max Forward Code Channels, Max Reverse Code Channels

Packet Data Registration
Link Establishment (PPP, RLP)

Active State

Inactivity Timer

Traffic Channel Release

Dormant State

Arrival of Layer 3 Data

Call Origination: Packet Data Service Option

Service Negotiation:
Max Forward Code Channels, Max Reverse Code Channels

Existing Packet Data Registration
Link Establishment (RLP)

Active State

Supplemental Channel Request Message (SCRM)

Pilot Strength Measurements, Data Backlog

Burst Level Admission Control

Supplemental Channel Assignment Message (SCAM)

Burst Length, Assigned Supplemental Code Channels, Action Time

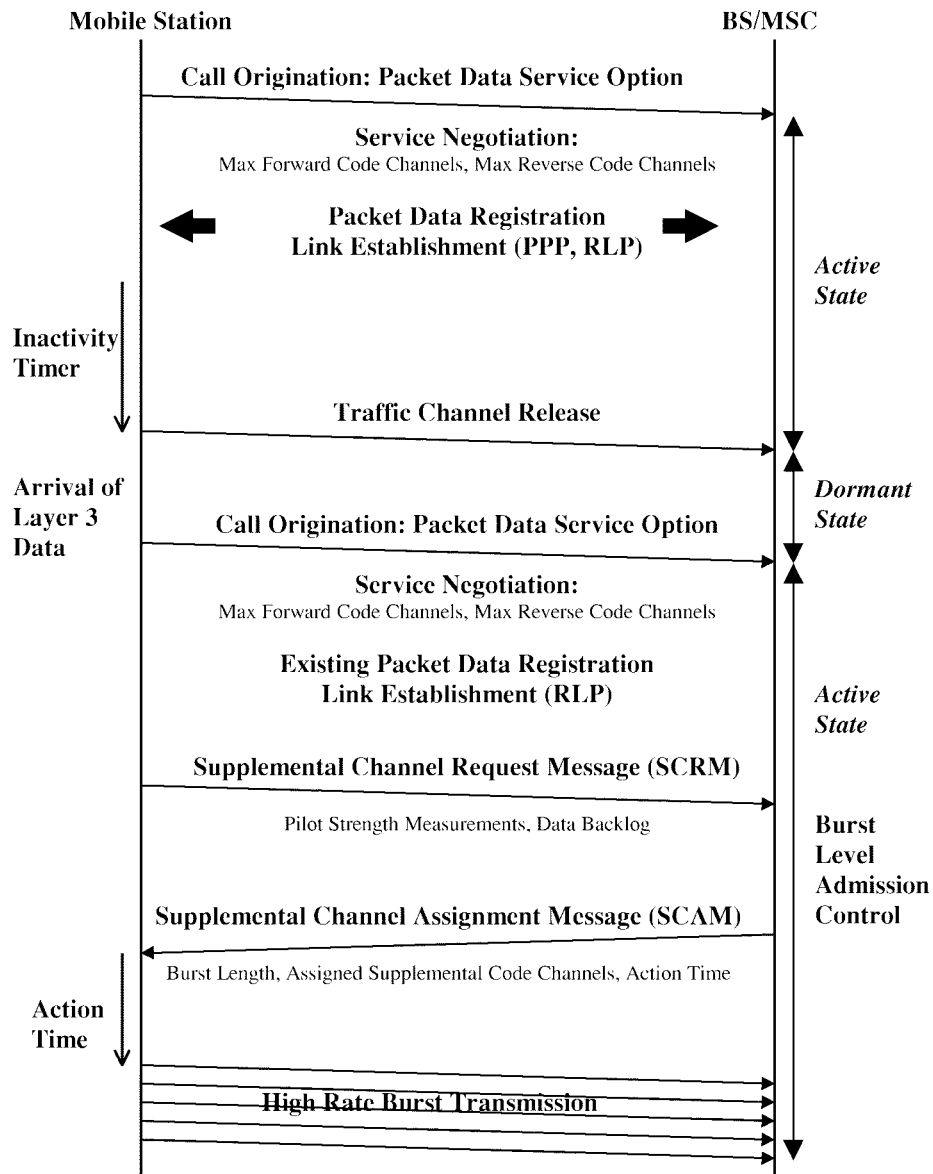Action Time

High Rate Burst Transmission

Fig. 4. Message flow for reverse burst access based on IS-95 Rev B messages.

there are ten voice users in a cell and the data user requests high-rate burst access. The data user is assumed to be at a point x on the line joining the two BS's. Fig. 2 shows the case when the path loss to both BS's is equal. Fig. 3 shows the case when the path loss to the neighbor BS is 6 dB higher corresponding to the high data-rate user being "closer" to one cell compared to the other. With equal path loss, 57.6 kb/s access is only permitted if the neighbor cell has fewer than 12 voice users. 38.4 kb/s access is permitted if there are fewer than 17 voice users and 19.2 kb/s access if there are fewer than 22 voice users. On the other hand, if the data user is away from the boundary (6-dB higher path loss to the neighbor cell), 57.6 kb/s access is permitted if the number of voice users at the neighbor cell is less than 24, otherwise 38.4 kb/s access is permitted.

III. PROPOSED SOLUTION

From the static interference analysis above, we conclude that the data rate the high data-rate user is permitted to transmit is a

function of its current path loss and shadow fading conditions to its connected cell as well as neighbor cells. Since the interference environment changes dynamically due to user mobility, it is convenient to define a burst mode for packet data service. High data-rate users are allocated "short" high data-rate bursts depending on the current interference and load conditions. Burst allocation is done through a message flow scenarios as described below.

A. Quiescent Mode

As shown in Fig. 4, an active high-rate mobile is assigned a fundamental code channel on origination. Parameters of the high data-rate service are negotiated at that point. The mobile then goes into a quiescent mode if it has no data to transmit. When a user is quiescent, a very low rate (say, eighth rate) signaling channel is maintained using its fundamental code. This sub-rate channel helps in maintaining synchronization and coarse power control. It is maintained whether the user

is "connected" to one BS or is in soft handoff with multiple cells. This fundamental code channel also serves as a fast, dedicated signaling channel for high data-rate service.

B. Burst Access Request

The synchronization and power control are inadequate if the quiescent period is long. Hence, the first one to two frames transmitted after a long quiescent period may be lost. This can be easily fixed by requiring the transmission of one (or more) idle basic rate frame at the end of a "long" quiescent period. Following these full rate idle frames that give the receiver time to synchronize and provide power control feedback, data transmission can begin. On the reverse channel, the mobile may signal on the fundamental code channel, requesting a higher data-rate burst transmission opportunity by indicating to the BS its data backlog. On the forward link, the BS may signal the mobile on the fundamental channel to prepare to receive a higher data-rate burst transmission.

The burst access request from the mobile contains the data backlog and the maximum data rate requested. The maximum burst length that may be requested is specified by the system (and is chosen to best coordinate shared access between users). In addition, to assist the BS in deciding if this burst request can be accepted without affecting QOS for other users, the mobile includes pilot strength information for cells in its neighbor list within the access request. The pilot strength measurements received from the mobile indicate to the BS the interference levels that will be seen at the BS and its neighbors due to transmissions from the mobile. In particular, the higher data rate user will be granted a burst request only if this transmission will not affect the QOS of active users in all cells.

For forward link burst transmissions as well, the BS may request the mobile to report pilot strength measurements prior to burst allocation. The network can use these measurements for power allocation and to determine the interference seen at the mobile, when the loading in adjacent cells is unequal. As discussed below, pilot strength measurements may also be used by the network to choose the subset of legs to allocate for higher data-rate burst transmission to the mobile.

C. Access Control Mechanisms

Once the burst request is received at the BS, the network must coordinate access with other burst requests as well as with the voice load already offered to the system. Access control mechanisms may be defined with varying amounts of complexity. The simplest is implemented autonomously by each BS. On the forward link, this is done by constraining the maximum transmitter power at each of the cells/sectors. On the reverse link, the admission algorithm can be based on limiting the minimum attenuation from the mobile to the cells it could potentially interfere with. Coordination across cells is still necessary in the burst allocation stage to assign resources at the soft-handoff legs.

More general procedures require access coordination between neighbor BS's including sharing load information among neighbor cells. Unlike autonomous schemes, light

loading in neighbor cells can be exploited in this case to permit higher rate access while still meeting the interference constraints. These methods are discussed in Section IV.

D. Number of Legs for Supplemental Channels

When the mobile is in soft handoff on several legs, it may be desirable to limit the number of legs on which supplemental channels are transmitted. This scheme has the following benefits.

1) It saves network resources.
2) It reduces messaging during supplemental channel setup.
3) It saves RF resources on the forward link as fewer active cells need to expend power in transmitting the supplementals; there is no such capacity benefit on the reverse link, where the mobile uses up RF resources at those cells while not benefiting from the soft handoff gain.

However, this comes at the cost of the mobile losing the benefit of soft-handoff on the supplemental channels. For IS-95B-based systems, the power control on the supplemental channels is done based on the fundamental which benefits from soft handoff. Because of this, the supplementals may see a poorer performance when they do not have the same soft-handoff benefit as the fundamental channel. For high-mobility users, the resulting performance without the benefit of soft handoff may not be acceptable. These tradeoffs are studied in this paper in Section VI-C.

The situation is worse on the forward link than on the reverse link. Consider a scenario where the mobile is moving from BS 1 to BS 2. Also assume that BS 1 is strong at the time a request for supplemental channels is made and hence the supplementals use only BS 1. When BS 2 gets strong, the fundamental, deriving the benefit of soft handoff, would require smaller power. The reduction in transmit power from BS 1, together with the increase in interference when approaching BS 2, would lead to unacceptable performance on the supplementals. Note that the reverse link does not see this increased interference.

E. Forced Termination of a Burst

The above mentioned admission control algorithm is based on the information available at the time of decision. Conditions may deteriorate during the course of a burst due to user mobility or change in voice loading. Since packet data can tolerate variable delays and bandwidth, we can protect voice users through forced termination of bursts based on some quality measure, for example, the FER on supplementals.

F. Mobility Metric

User mobility imposes many constraints on the system. For example, an active user has network resources allocated, even when not in burst transmission. When this user moves to an adjacent cell, it is allocated new resources to keep it in the active state. There is a large infrastructure overhead associated with signaling and reallocation/deallocation of resources for such a user. The overhead is larger if bursts are continued

across handoff events. This overhead is a function of user mobility.

When a mobile data user in burst transmission mode generates a new handoff add trigger, that may be an indication of the mobile approaching a new sector/BS. In addition to allocating resources at the new cell, the interference caused by the high-rate mobile also need to be re-evaluated. Because of these constraints, it may be practical to terminate the burst or drop down to a lower rate at an add trigger. New burst assignment could be made based on the resource availability and interference constraints after the handoff is completed. The mobility of the user determines the rate of such triggers, and along with the burst length determines the probability of forced termination of bursts.

The length of the burst and number of codes assigned to a packet data user could be made a function of user mobility. Fixed- or low-mobility users may be assigned higher number of codes for longer durations than high mobility users. Low-mobility users may also be assigned supplementals on fewer legs than the fundamental channel so as to save on the resources. The mobile's handoff activity is an excellent mobility metric that directly relates to the issues discussed above. A running average of the number of handoff events by a mobile can be used to optimize the resource usage by assigning number of codes per burst and burst durations appropriately.

IV. BURST ADMISSION ALGORITHMS

Burst admission algorithms [16] with various levels of complexity can be defined. We discuss simple algorithms in this paper. More complex procedures and mapping to distributed architectures is left to the system designer. For simplicity, we describe the control procedures with a single data user.

We start with the assumption that the fundamental channel for the high-speed data user is already established. We then explore admission control algorithms for assigning supplemental channels to users on demand.

A. Forward Link Assignment Algorithm

Consider mobile j in cell (sector) k. k could be any of the active BS's with which the mobile is in soft handoff. Assume that this mobile is using power $P_{j,k}$ on the fundamental code channel and that current forward link load in cell k is L_k. Also assume that the maximum permitted load in cell k is $L_{k,\max}$.

Under the above assumptions, it is permissible to assign mobile j, m_j supplemental code channels if

$$L_k + m_j P_{j,k} \leq L_{k,\max}, \text{ for all cells } k \text{ with which}$$
$$\text{the mobile is in soft handoff.} \qquad (7)$$

This assumes that all supplemental code channels require the same transmit power per channel as the fundamental code channel $P_{j,k}$, and that the power of all other users is unchanged following the addition of the supplemental channels.

Several enhancements are possible.

1) The FER on the supplementals can be traded off by transmitting the supplementals at a lower power than the fundamental. For packet data services, the errored frames can be recovered through retransmissions. We find that this can have a resultant capacity gain.
2) The threshold $L_{k,\max}$ can be dynamically adjusted as a function of the load at neighbor cells $L_{k'}$ to exploit low neighbor loads. This enhancement requires communication of forward link loads between BS's.
3) When the mobile is in soft handoff, for the burst duration the supplementals are assigned on a subset of legs on which the fundamentals are active. At burst allocation, the mobile is requested to reports pilot strengths and the burst is allocated on a subset of legs that have the strongest pilots.

Some of these methods emerged in our deliberations in the standards working group TR 45.5.3.1 of the Telecommunications Industry Association (TIA). In particular, credit for proposing that the burst could be assigned on a subset of active legs should go to Qualcomm.

B. Reverse Link Assignment

Reverse link burst admission algorithm is more complex. Unlike the forward link, reverse link burst allocation always requires that interference constraints at neighbor cells be satisfied. For the active cells (i.e., cells with which the high-speed data mobile is in soft handoff), we allocate radio resources according to the analysis discussed next. For simplicity, the analysis below assumes equal size cells with equal pilots. The analysis can be easily extended for unequal cells.

We describe a simple admission algorithm at active cells, assuming that the following measurements are available:

1) measurement of total received power at BS;
2) reverse link E_b/N_0 measurements for the fundamental channel of the jth mobile at each of the legs with which it is in soft handoff.

The total received power R_k can be written as

$$R_k = \sum_j X_{jk} + I_{\mathrm{oc}} + N_o \qquad (8)$$

where X_{jk} is the received signal power at cell k from the jth mobile, where j is summed over the set of mobiles that have cell k in their active set, and I_{oc} is the other cell interference. X_{jk} can be written in terms of the received E_b/N_0 for user j at cell k and the processing gain G as

$$X_{jk} = \frac{1}{G} R_k \left(\frac{E_b}{N_0} \right)_{jk}. \qquad (9)$$

The admission algorithm is to allow N_j supplementals to mobile j if the resulting total power estimate falls below a threshold, i.e.,

$$R_k + N_j X_{jk} \leq \text{Threshold} \qquad (10)$$

at each of the legs k with which the mobile is in soft handoff (active and candidate cells).

It is also necessary to evaluate the interference at the nonactive cells caused by the admission of a burst. This is done as follows. Let S_{jk} denote the pilot strength at mobile j

of pilot from cell k. Define the largest reported pilot strength that is not in the active or candidate set as

$$S_{k_1(j)} = \max_{k \text{ not in active or candidate set}} S_{jk}. \quad (11)$$

Then, to avoid causing excessive interference at cell $k_1(j)$, the "nearest" nonactive neighbor, the burst request is denied if its reported pilot strength is larger than a "burst admission" threshold T_{burst}

$$S_{k_1(j)} > T_{\text{burst}}. \quad (12)$$

An alternate criterion that accounts for the difference in path loss to the active and nonactive BS's is as follows. Define the largest reported pilot strength that is in the active or candidate set as

$$S_{k_0(j)} = \max_{k \text{ in active or candidate set}} S_{jk}. \quad (13)$$

Then, to avoid causing excessive interference at cell $k_1(j)$, the burst request is denied if

$$S_{k_0(j)} - S_{k_1(j)} < \Delta_{\text{burst}}. \quad (14)$$

Here Δ_{burst} is chosen to account for the path loss difference between the strongest active and strongest nonactive pilots.

V. Performance Analysis Methodology

In order to study the performance of the burst admission algorithms described in Section IV, we have used a combination of static and dynamic simulation approaches.

Coverage-related issues are addressed through the use of static modeling as in [8], [9]. In these models, outage (referred to as static outage in the sequel) is defined as the signal to interference ratio (SIR) falling below a given threshold. Coverage and capacity can be determined through analysis, assuming that mobile densities and fading models are analytically tractable. Alternately, Monte Carlo simulations can be used to make outage calculations.

These static models do not capture the time correlations of the signal due to fading and mobility. In order to study the performance seen by the high data-rate user, it is important to understand the impact of variation of the environment on the performance of the call. Burst admission probabilities and performance during bursts cannot be captured in static outage results.

Dynamic simulations are critical to capture performance at the call level. For example, even if the received signal level becomes unacceptable for a short duration, it may be acceptable from the perspective of a call if the duration of the fade is short enough. That is, the outage that affects call performance is the SIR falling below a certain threshold for a given duration τ_m. Fade and outage durations are a function of the fading environment and mobile speed. Similarly, handoff timers and handoff delays also impact the QOS. These effects can not be captured by the traditional static models, which are amenable to analysis. Recent work on on analysis of "minimum duration outage" [19] based on level crossing theory is of some interest in this regard.

In interference-constrained CDMA systems, to obtain meaningful results it is necessary to simulate a system with several rings of cells. With wider bandwidths and multiple classes of users, soon the number of mobiles, and the number of parameters, explodes. A detailed simulation of such a system, including the dynamic RF propagation environment, is very time consuming and does not allow much insight into the tradeoffs. We propose and use a hybrid analytical/simulation-based approach [14] to study the system performance with integrated services as discussed below. This simulation allows us to study various admission algorithms and their impact on system capacity.

A. Static Simulations

We use static Monte Carlo simulations to obtain the coverage plots for high-speed data. The simulation environment consists of a hexagonal grid with BS's located at the center of every hexagon. The BS's are assumed to be sectorized with three sectors and realistic antenna patterns. A mobile is introduced at a position that is uniformly distributed over the coverage area. The signal attenuation seen by the mobile has two components: distance loss and shadow fading. The distance loss is taken as $d^{-\delta}$, where δ is the propagation constant. Shadow fading is modeled using the Mawira model [18], which simulates an urban environment.

Using this path loss we determine the E_c/I_o corresponding to all the pilots. The mobile is assumed to be in soft handoff with all the BS's whose pilot strengths exceed the threshold T_{Add}. For studying the forward link performance in soft handoff, we assume selection diversity. We also assume perfect power control so that the transmit power is able to completely compensate for the distance and shadow fading loss to the "closest" BS in terms of path loss. The number of supplemental code channels assigned to the mobile on the forward link can be determined from the required E_b/N_0 and the neighbor cell interference.

For the reverse link, a burst is admitted if the burst admission criteria described in (12) or (14) are satisfied. If the burst is admitted, the number of supplemental code channels assigned to the mobile on the reverse link is further limited by the mobile transmit power constraints.

Over a large number of Monte Carlo trials of this simulation, the fraction of trials in which a burst is admitted can be determined, or a given number of supplementals can be assigned that satisfy the interference and transmit power constraints. This provides static coverage results.

B. Dynamic Simulation Description

The static simulation described above is enhanced as follows. The same simulation environment consisting of a hexagonal grid with three sectored cells is used. The macro behavior of one mobile is simulated in detail. Shadow fading is modeled using the Mawira model [18], which simulates an urban environment. It is the sum of two independent lognormal components v and w, each with an exponential correlation function as suggested in [17], but with different correlation distance and variance. The first component, v, has large variance and

short correlation distance, and the second component has a small variance with large correlation length. In particular, we have used standard deviations: 5.4 and 4.2 dB and correlation lengths 100 and 1000 m, respectively. The path loss exponent is $\delta = 4$.

The mobile chooses a random starting location (Uniform over the cell) and direction of motion (Uniform over [0,360]) at the beginning of the call. It traverses in a straight line until the call is completed. Call holding time and the speed of the mobile are taken to be constant. The position update of the mobile as well as the handoff evaluation are carried out at 100-ms intervals. Unless specified explicitly, we assume the mobile speed is fixed at 35 mi/h.

During the length of the call, the mobile monitors the pilot signal to interference ratio and does handoff evaluation using the algorithm specified in IS-95 with parameters $T_{\text{Add}}, T_{\text{Drop}}$, and $T_{T_{\text{drop}}}$. The network delays in effecting a handoff add/drop are assumed to be constant (1 s). If, after going through the handoff evaluation sequence, the mobile finds all its active pilots dropped, the call is assumed dropped due to pilot loss. The parameter values used for the results in the following sections are: $T_{\text{Add}} = -12$ dB; $T_{\text{Drop}} = -16$ dB; and $T_{T_{\text{drop}}} = 3$ s.

We assume perfect power control for these simulations. The supplementals and fundamental code channels each use identical transmit power. The impact of realistic (fast) power control on the reverse link is studied separately in Section VIII.

In the reverse burst mode, the data mobile makes a reverse burst request to send a burst every R_{burst} s. This request includes the pilot strength measurements made by the mobile. The mobile request is admitted after a delay of D_{burst} s if the burst admission criterion is satisfied (see Section IV-B). Otherwise the burst is denied. Burst transmission is interrupted at a soft handoff add trigger.

In the forward burst mode, a request for a forward burst arrives every R_{burst} s. The mobile is requested to report its pilot strength measurements to determine burst admission as discussed in Section IV. The burst is admitted after a delay of D_{burst} s. Burst transmission is interrupted at a soft handoff add trigger. We use $R_{\text{burst}} = 4$ s and $D_{\text{burst}} = 1$ s in all the simulations in this paper.

The simulation outputs the following burst performance metrics: fraction of the burst requests that are admitted; the average burst length; and the distribution of reverse link interference caused at each of the adjacent cells/sectors. The simulation outputs these statistics by averaging over a large number of calls.

C. Analysis of Reverse Link Interference

From the interference distributions caused by a single voice or data user at a single cell, we can obtain the distribution of total interference due to N_v voice users and N_d data users by convolving the corresponding distributions. Bounding the probability of interference exceeding a given threshold at a specified outage value gives us the tradeoffs and capacity achievable in terms of the number of voice and data users that can be supported.

Let us denote the probability density function (pdf) by p and corresponding distribution function by F. The pdf of the interference generated at each of the 19 cells by this single mobile is collected from the simulation described in Section V-B. These pdf's capture the randomness due to position of mobile, mobility, shadow fading, and burst activity and are computed for each of the following scenarios:

1) a full rate circuit-mode data mobile, $p_{d,k}$, where k denotes the cell index;
2) a mobile following the burst admission strategy described here, $p_{b,k}$.

Given that voice activity is independent of user mobility, the distribution of interference due to a voice user can be obtained from the corresponding expression for a circuit mode data user approximately as

$$F_{v,k}(x) \approx F_{d,k}(x/a) \tag{15}$$

where $F_{v,k}$ is the distribution function corresponding to $p_{v,k}$, the pdf for the voice user, and a is the voice activity. Similarly, the distribution corresponding to a circuit (burst) mode data user with M codes is $F_{d,k}(x/M)$ $(F_{b,k}(x/M))$.

We now use symmetry to obtain the distribution of total signal power generated at BS 0 when there is one mobile per cell. It can be seen that the distribution of interference caused at cell 0 by a mobile in cell k is the same as that caused at cell k by a mobile in cell 0. Using this argument, the distribution of received power at cell 0 due to one voice mobile in each of the cells can be calculated as

$$p_v = p_{v,1} \otimes p_{v,2} \otimes \ldots \otimes p_{v,K} \tag{16}$$

where $\otimes$ denotes convolution and K is the number of adjacent cells which contribute reverse link interference.

These pdf's are then further convolved to obtain the distribution of interference due to a given mix of voice and data users. That is, if there are N_v voice users and N_d packet-mode data users, then the resulting interference distribution on the uplink is obtained as

$$p(x/N_v, N_d) = (p_v(x) \otimes p_v(x) \otimes \ldots p_v(x))_{N_v}$$
$$\otimes (p_d(x) \otimes p_d(x) \otimes \ldots p_d(x))_{N_d}. \tag{17}$$

The expression for outage, defined as the probability of the total received power (or equivalently, rise above thermal noise) exceeding a threshold I_T can be computed from (17) as

$$P_{\text{out}}(N_v, N_d) = \int_{I_T}^{\infty} p(x/N_v, N_d) \, dx. \tag{18}$$

I_T is assumed to be the same for both data and voice users and is computed using the methodology described in [8]. Reverse link capacity results for high-rate data user using circuit mode versus burst mode are obtained using this hybrid method and are reported in Section VII-B.

Note: Our hybrid simulation/analysis approach is to build on elemental dynamic simulations of individual mobiles of different classes and captures the impact of these mobiles on all cells through the pdf of caused interference. The elemental simulations assume that the mobile power control compensates for the mean interference at the target cell. At uniform high

load the normalized variation in aggregate interference is small, hence the onset of outage, and therefore the capacity, is captured accurately.

D. Analysis of Supplemental Channel Performance

We can use the hybrid simulation model described here to study supplemental code channel performance when supplementals are allocated at a subset of the active set of legs on the fundamental code channel. The subset of legs is chosen based on the pilot strengths reported by the mobile. One or more BS's with the strongest pilot strengths are chosen for each burst. This ensures that the "best" active leg(s) are chosen at the time of admission of the burst. The fundamental channel continues to be assigned at all the active BS's.

Supplemental code channel performance may be obtained using the following analytical model. The transmit power for each leg is determined by the target E_b/N_{0_T} required to achieve the desired (1%) FER on the fundamental code channel. Since there is no separate power control on the supplementals, transmit power on the supplementals is determined by the power control on the fundamental. The FER on the supplementals is determined based on the subset of legs on which supplementals are allocated and the respective transmit power level.

In this paper we study a simplified version of the above analysis. We assume the following "soft handoff" model: the E_b/N_{0_T} required to achieve the desired (1%) FER is achieved on the leg with the highest SIR.[2] Since the supplementals are assigned on a subset of the active legs, the highest SIR among this subset will be smaller than (or equal to) the SIR achieved on the fundamental (all active legs). This difference in SIR (δ_{supp}) is the loss in E_b/N_0 on the supplementals compared to the target. The FER on the supplementals is determined at $E_b/N_{0_T} - \delta$ from a look-up table.

This method of determining FER performance when supplementals are allocated on a subset of active legs is equally valid for the forward and reverse burst allocation. Gains from equipment blocking, burst assignment complexity, and delay reduction are applicable to both links; the capacity advantage is applicable only to the forward link.

VI. FORWARD LINK CAPACITY AND COVERAGE

A. Forward Link Capacity

Consider the scenario of equal sized (sectorized) cells. All cells are assumed to have the same maximum transmit power determined to provide sufficient coverage at capacity for a voice-only system. A forward link E_b/N_0 requirement of 7 dB is assumed. The orthogonality factor, which is the fraction of the total transmitted power on the forward link that is seen as interference by each of the codes from the same cell, is assumed to be 10%. Note that if all the codes at the receiver are orthogonal, the factor should be 0%. Multipath delay spread results in reduced orthogonality.

[2] Better models of soft handoff gain will result in more accurate results for supplemental code channel performance. This work is currently in progress.
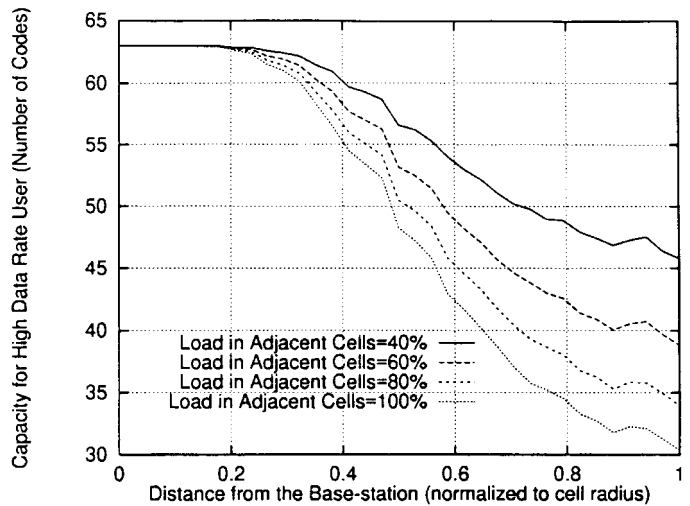

Fig. 5. Forward link capacity: number of codes available to the high data-rate user as a function of distance from the BS.
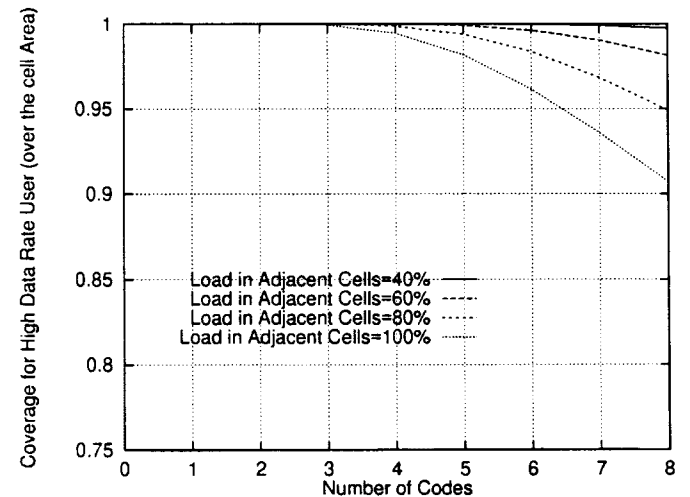

Fig. 6. Forward link coverage: coverage area versus number of codes.

Fig. 5 shows the capacity (number of codes) available on the forward link as a function of the distance of the user to the BS. These results are obtained from the static simulations described in Section V-A. The plots are parameterized by the load in the neighbor cells (percentage of maximum transmit power). The neighbor cell load may come from a mix of voice and data users. Thus, increasing load in the neighbor cells results in increasing interference to users at the boundary and reduces the available capacity. The results show that with the environment assumed, enough capacity exists in a cell to support multiple high data-rate users. Even at the edge of the cell, when fading and interference conditions are favorable, a high number of codes can be allocated to the data user. However, as we will see next (Fig. 6), this large capacity cannot be made available under coverage guarantees.

A lower E_b/N_0 requirement, as in the case of stationary mobiles, translates to even higher capacity and coverage, whereas a higher E_b/N_0 requirement seen, for instance, during unfavorable fading conditions leads to a reduction in the capacity and coverage.
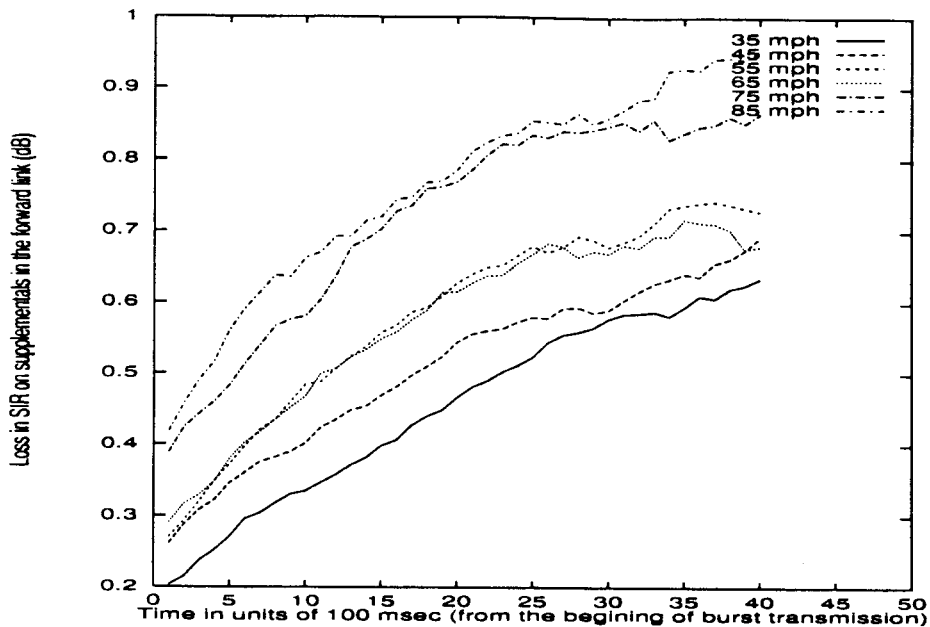
Fig. 7. Average loss in power with a single supplemental leg.

B. Forward Link Coverage

We use the same model as above: required $E_b/N_0 = 7$ dB, orthogonality factor between Walsh code channels within the same cell $= 0.1$ and a maximum power constraint for the cell. In Fig. 6, we show the percentage of cell area over which high data-rate service equivalent to M times the basic rate can be provided. There are no other voice users in the cell and the plots are parameterized by the load in other cells. Fig. 6 shows that interference constraints permit up to eight times the basic rate over 90% of the coverage area even when the adjacent cells are fully loaded. We note that for good coverage, only a fraction of the available capacity found above can be exploited. A burst-mode scheme that assigns the resource (transmit power) based on the user's E_b/N_0 requirement, path loss, and interference condition is required for best utilization of the available capacity.

C. Supplemental Channel Performance

We use the performance analysis methodology described in Section V-D to address the question of assignment of supplemental code channels on a subset of active legs. Although this feature is applicable to both the forward and reverse links, this is primarily a forward link enhancement with potentially large capacity gains. As discussed in the analysis, our simplified model assumes that the SIR seen on the fundamental channel is given by the highest pilot signal to interference ratio received among all the active legs.[3] The SIR seen on the supplemental code channel is the highest pilot SIR received among the subset of pilots on which the supplementals are allocated.

1) Supplemental Channels Assigned on Only One Leg: Assigning supplemental channels at one BS saves network resources and greatly simplifies handling of bursts. Supplemental code channels are assigned at the start of the burst

---

[3]This is an approximation. Better models of maximal ratio combining will give more accurate results.

---

at the leg with the largest pilot. Bursts are terminated on handoff triggers as handoff events may deteriorate the quality of the burst transmission. The average ratio of the SIR of the fundamental to supplemental is collected at 100-ms intervals during the burst. As shown in Fig. 7, this ratio increases as the burst progresses and is higher for higher mobile speeds. The average loss in SIR over the 4-s duration of the burst is less than 1.0 dB, even at the high mobile speeds.

The loss in SIR can be translated to an increase in FER using a look-up table of E_b/N_0 versus FER. The results here are for Rate Set 2 and 2 RAKE fingers. From the table look-up we find that at 65 mi/h, a loss of 0.5 dB in SIR results in an increase in FER from 1–2%, while a loss in SIR of 1.33 dB results in an increase to 5%. We may conclude that when the FER on the fundamental is maintained at 1%, even at 65 mi/h, on average the FER on the supplementals exceeds 2% after 1.5 s of the burst and does not exceed 5% for the burst duration (of 5 s). Since the average loss in SIR is less than 1 dB, we may also conclude that by increasing the power of the supplemental channels by 1 dB we can keep the average FER across bursts below 1% for all speeds. However, the average loss in SIR may be misleading, since a fraction of bursts suffer large loss.

We next estimate the probability of a burst transmission experiencing high FER by obtaining the probability distribution of supplemental channel SIR for all bursts. The distribution of the difference in SIR is plotted for different speeds and presented in Fig. 8. The SIR values are taken at intervals of 0.1 s during every burst, and a distribution is obtained from simulation of 1500 calls. We have also shown the point on the plots corresponding to FER hitting 5% on the supplementals for two cases: 1) when the supplementals are transmitted with the same power as the fundamental and 2) when the supplementals are transmitted with power 1 dB greater than the fundamental. From Fig. 8 we see that percentage of instances when a burst encounters an FER greater than 5% is 2.4% for a speed of 5 mi/h and increases to 9% for a speed of 65 mi/h. By
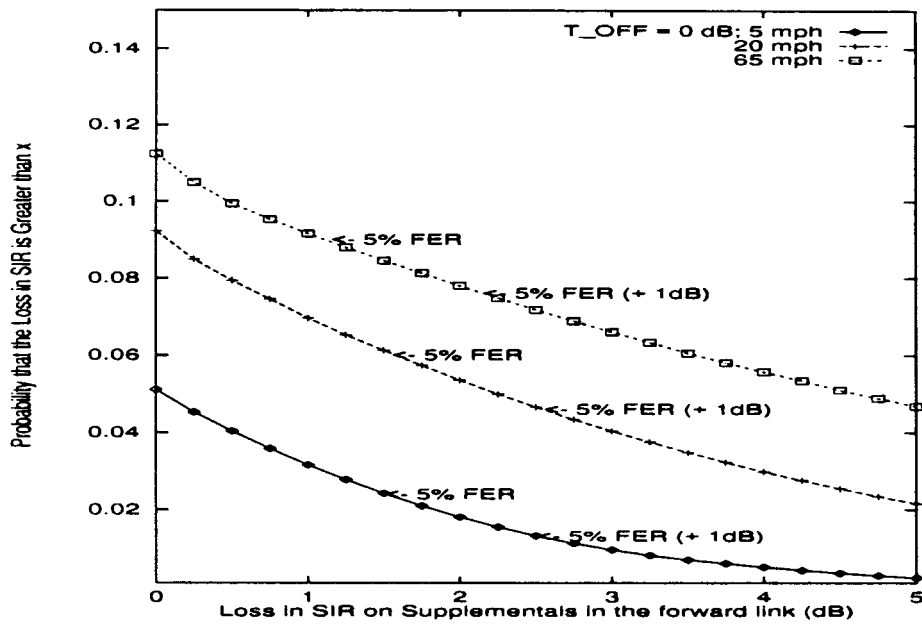
Fig. 8. Probability of the loss in SIR exceeding a given value with a single supplemental leg.

increasing the transmit power on supplementals, these numbers can be reduced to 1.8 and 8%, respectively.

We conclude that increasing the power on the supplementals for all bursts provides a small improvement in the percentage of bursts that see high FER. Although from the average FER results in Fig. 7 we had concluded that increasing the power of the supplemental channels by 1 dB can keep the average FER across bursts below 1% for all speeds, we now see that this strategy does little to help the bursts that see outage. Additional procedures must be defined to identify such outage conditions and to terminate specific bursts that see degraded performance.

2) Supplemental Channels Assigned on a Subset of the Active Set: We now study the performance when the supplemental code channels are assigned to a subset of legs in the active set. Our proposed algorithm is to choose the subset such that the pilot strength of the chosen BS's is within T_{OFF} of the best leg (with the highest pilot strength). The SIR seen by the supplementals will be the maximum of the SIR's among the subset. As the burst progresses, the probability that the best leg on the fundamental is active on the supplementals is higher for this case than the case where the supplementals are allocated on exactly one leg. Moreover, the probability of receiving high SIR on the supplementals increases with the cardinality of the subset, which increases with increasing T_{OFF}.

We collect statistics on the instances that the supplementals encounter FER exceeding 5 and 10%. We also collect statistics on the percentage of bursts that encounter FER exceeding 2, 5, and 10% FER at least once during the burst duration. These statistics are presented in Tables I and II, respectively. Note that $T_{OFF} = 0$ dB corresponds to supplementals being allocated on exactly one leg. We see that at 5 mi/h, 6.1% of the bursts encounter an FER of 5% or more when a single leg is used for the supplementals. From Table I we find that across all bursts, an FER of 5% is exceeded in 2.4% of the instances. By increasing T_{OFF}, the percentage

TABLE I
PERCENTAGE OF INSTANCES WITH LARGE FER FOR A 4-s BURST

SPEED (mph)	FER	T_{OFF}				
		0	1 dB	2 dB	4 dB	6 dB
5	> 5%	2.40	1.30	0.60	0.17	0.05
	> 10%	1.70	0.90	0.48	0.11	0.03
20	> 5%	6.00	4.50	3.40	1.65	0.75
	> 10%	5.10	3.75	2.75	1.25	0.58
65	> 5%	9.00	8.40	6.75	4.30	2.85
	> 10%	8.50	7.75	6.25	4.00	2.60

TABLE II
PERCENTAGE OF BURSTS EXCEEDING REQUIRED FER FOR A 4-s BURST

SPEED (mph)	FER	T_{OFF}				
		0	1 dB	2 dB	4 dB	6 dB
5	≥ 2%	7.67	5.18	3.12	1.10	0.32
	≥ 5%	6.12	3.90	2.12	0.57	0.13
	≥ 10%	4.72	2.86	1.60	0.35	0.11
20	≥ 2%	14.30	11.84	9.61	5.95	3.31
	≥ 5%	12.85	10.61	8.41	4.93	2.35
	≥ 10%	10.82	8.67	6.83	4.04	2.05
65	≥ 2%	18.85	16.86	14.64	10.90	7.58
	≥ 5%	17.06	15.18	13.26	10.36	7.22
	≥ 10%	16.52	14.67	12.97	9.81	7.09

of bursts that see FER exceeding 5% can be reduced to 3.9% ($T_{OFF} = 1$ dB) and 0.1% ($T_{OFF} = 6$ dB). At 20 mi/h and T_{OFF} varying from 1–6 dB, the probability of encountering an FER above 5% decreases from 4.5–0.75%; the percentage of bursts encountering 5% FER decreases from 10.61–2.35%. By increasing T_{OFF}, the signal quality during bursts can be improved significantly at the cost of increasing the number of legs on which supplementals are assigned. Thus there is a tradeoff with capacity as discussed next.

3) Forward Link Capacity Gain: As T_{OFF} increases, the average number of legs on which supplementals are allocated increases, and consequently the supplemental SIR improves.

TABLE III
COMPARISON OF CAPACITY GAIN

Speed (mph)	T_{OFF}	Average Number of Fund. Legs	Average Number of Suppl. Legs	Capacity Gain
5 mph	1 dB	1.91	1.10	42%
	2 dB	1.91	1.19	37%
	4 dB	1.91	1.39	27%
	6 dB	1.91	1.59	16%
20	1 dB	2.02	1.08	47%
	2 dB	2.02	1.17	42%
	4 dB	2.02	1.37	32%
	6 dB	2.02	1.57	22%
65	1 dB	2.10	1.08	49%
	2 dB	2.10	1.16	45%
	4 dB	2.10	1.33	37%
	6 dB	2.10	1.51	28%

The total transmit power increases with the number of legs allocated for the supplementals. By using a smaller T_{OFF} and fewer legs on the supplementals, the reduction in transmit power can be translated into a capacity gain at the cost of worse FER performance on the supplementals. Table III shows the percentage capacity gain for different values of T_{OFF}.[4] At 5 mi/h with $T_{\mathrm{OFF}} = 1$ dB, the average number of supplemental legs is 1.1. Hence the capacity gain is 42% compared to the system with an average number of supplemental legs equal to 1.91, the same number of legs as the fundamental channel. At 65 mi/h, with $T_{\mathrm{OFF}} = 1$ dB, the gain is 49%. The capacity gain is with respect to the case when the supplementals are allocated on all active legs and achieve 1% FER. The degradation in FER performance was discussed above.

The capacity gain is the largest when a single supplemental leg is used. As discussed earlier, to improve the quality of the signal, the supplementals may be transmitted with increased power. At 5 mi/h, an increase in power of 1 dB (26%) reduces the percentage of instances when a bursts encounters 5% FER from 2.4–1.3. The same improvement in burst performance can be achieved with additional legs with $T_{\mathrm{OFF}} = 1$ dB (Table I). The average number of legs in this case is 1.10 (Table III). With equal transmit power on all the legs, the additional power expended is thus 10%. Thus, if additional power is to be expended to improve supplemental channel performance, it is better to allocate supplementals on additional active legs rather than just increase the power. Soft handoff on supplementals provides additional power only to bursts that require it, rather than across the board to all supplementals, and thus it provides more efficient use of power and consequently higher capacity.

4) Observations on Supplemental Code Channel Assignment: We have studied the assignment of supplementals on one or a subset of the active legs. The following conclusions are drawn.

1) Performance with a single supplemental leg is acceptable at low speeds. If 5% FER is considered acceptable for packet data service, 83% of bursts do not need multiple legs at a speed of 65 mi/h, while 94% of bursts do not need multiple legs at 5 mi/h.

---

[4]For a fair comparison, the gains must be discounted by the increase in the average FER across all bursts. Thus the capacity gains in Table III are somewhat optimistic.

2) Increasing the number of legs on which supplementals are assigned, through a choice of $T_{\mathrm{OFF}} = 1$ or 2 dB, still gives a substantial capacity gain with a significant decrease in percentage of bursts that exceed 5% FER. However, at higher speeds (65 mi/h), this percentage is still quite large and for good performance, and supplementals must be assigned on all legs.

Note: These results are based on a simple model of diversity where the performance is determined by the total received power from all legs. In reality, this diversity gain is a function of the relative attenuation of different legs in soft handoff and the multipath environment. In hostile environments, for example, when the mobile sees single path Raleigh fading, the soft handoff diversity gains are significant and it may be better to have the supplemental channels in soft handoff. Better models to capture the diversity gain under fading conditions and their impact on supplemental channel assignment are the focus of current simulations.

VII. REVERSE LINK COVERAGE AND CAPACITY

A. Reverse Link Coverage

The reverse link coverage depends on the burst admission algorithm and the mobile transmit power limitations. In this section, we capture the coverage assuming no mobile transmit power limit. The impact of mobile transmit power limitations is addressed in Section VII-C.

The algorithm described in (14) is used to decide on burst acceptance. The mobile provides neighbor pilot strength measurement results to the network as part of its burst request. The infrastructure denies the burst request if the expected interference caused at neighboring cells is too high. We assume that there are enough resources available at the target cell sites to allocate the burst if the interference conditions are satisfied. The admission algorithm provides tradeoffs between coverage and capacity through parameter Δ_{burst}. The capacity results and the corresponding tradeoffs are discussed in Section VII-B.

A plot of coverage as a function of distance from the BS, obtained from static simulations (Section V-A), is plotted in Fig. 9. These static simulation results accurately capture the burst admission trends as a function of distance and Δ_{burst}. The true admission probabilities also depend on system dynamics, including handoff events, and are captured in the dynamic simulation results in Section VII-B. The curves show that burst acceptance is high close to the BS, decreasing as the mobile approaches the edge of the cell. The admission probability also reduces as Δ_{burst} increases, decreasing to around 0.85 at the edge of the cell for $\Delta_{\mathrm{burst}} = 6$ dB. By reducing Δ_{burst}, the admission algorithm is relaxed. However, this would result in larger out-of-cell interference and penalty on the capacity available to the voice users (Section VII-B).

B. Reverse Link Capacity

In this section, we present reverse link capacity and outage results obtained from the dynamic simulation methodology
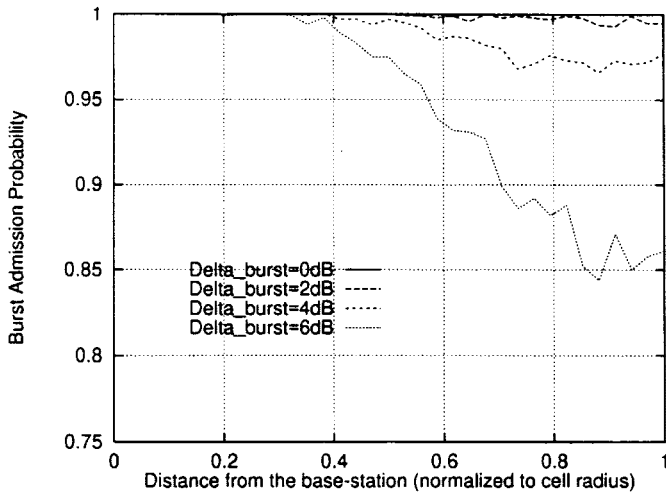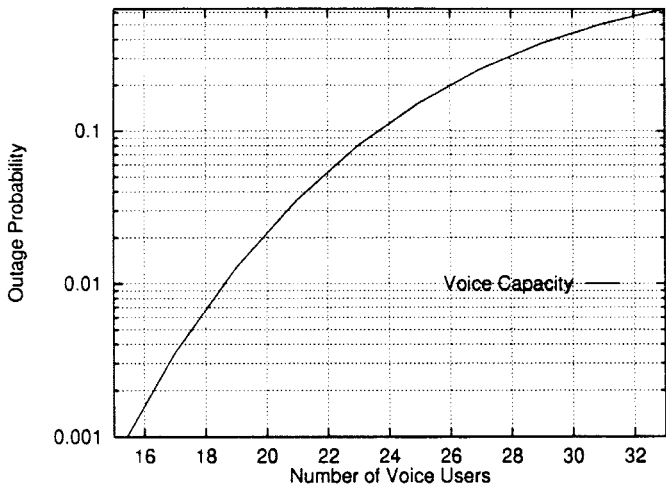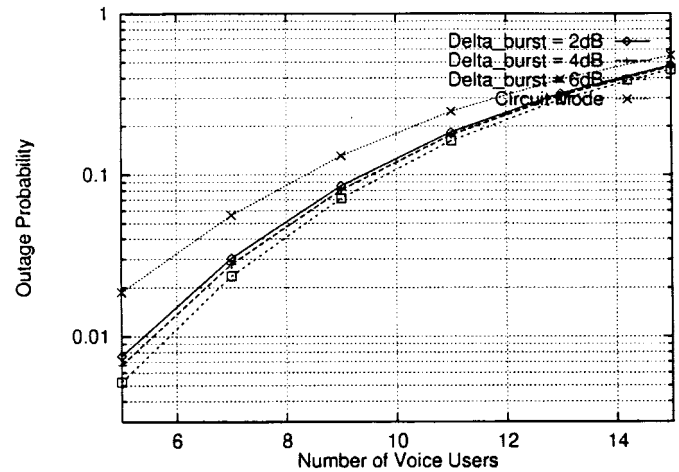
Fig. 9. Reverse link admission probabilities.

Fig. 11. Outage with one high data-rate channel at 57.6 kb/s (one high-rate data user is assumed to be active at any given time): impact of threshold Δ_{burst} on voice capacity.

Fig. 10. Outage of the system with only voice users.

TABLE IV
ADMISSION PROBABILITIES FOR DIFFERENT VALUES OF Δ_{burst}

Δ_{burst} (dB)	Admission Probability
2	0.88
4	0.84
6	0.77

Observations:

1) From Fig. 11, we observe that when the data user is operating in circuit mode, the system can support 6.8 voice users at 5% outage. Since the six codes corresponding to the data user are active all the time, the data throughput on each of those codes is approximately $1/\text{voice\_activity} = 2.2$ times higher than that of a voice user, on the average. This gives an equivalent total throughput of $6.8 + 2.2 \times 6 = 20$ voice users when there is one circuit mode data user active. It translates to a loss of 9% in throughput, compared with the voice-only system.

2) In burst mode, the burst admission control strategy ensures that the data users that cause excessive interference at the neighbors are not admitted. This results in higher capacities than is the case with circuit mode data. For the range of parameters considered in Fig. 11, we see that the capacity penalty can be almost completely eliminated (that is, throughput is $8.4 + 2.2 \times 6 = 21.6$ voice users for $\Delta_{\text{burst}} = 6$ dB).

3) Increasing Δ_{burst} reduces the outage experienced by the voice users. But this also limits the region over which high data rate service is available. For instance, if $\Delta_{\text{burst}} = 0$ dB, the burst request is never denied. As Δ_{burst} is increased from 2–6 dB, the coverage for 57.6 kb/s service shrinks from 88–77%.

The simulation results indicate that high data rate service can be provided over 75% of the area through a simple scheme that only looks at the local measurements made by the mobile. Better coverage over area can be achieved through using lower values for Δ_{burst} and taking a hit on the voice capacity.

described in Section V-C. Fig. 10 shows the outage of the system as a function of the number of voice users. It can be seen from this plot that the capacity of the system is 22 voice users per sector at 5% outage and 18.5 voice users at 1% outage.

In Fig. 11, we plot the outage experienced when there is one data user per sector operating in either circuit or burst mode at 57.6 kb/s (for example, thorugh six codes aggregated, each at 9.6 kb/s). The circuit mode data user is active with activity factor = 1. Alternately, there is one burst-mode data user active at any given time. No time is assumed to be lost in switching between bursts to different burst-mode data users, so that the shared high-rate burst-mode channel also has an aggregate activity factor = 1. This (100% efficiency) corresponds to the worst-case interference and highest throughput for the burst mode channel. The burst-mode data user follows the burst access scheme, with admission delay $D_{\text{burst}} = 1$ s, and burst length of 4 s. Fig. 11 is parameterized with the burst threshold Δ_{burst} (14). Table IV shows the corresponding probability of burst admission for high data rate service as a function of Δ_{burst}.
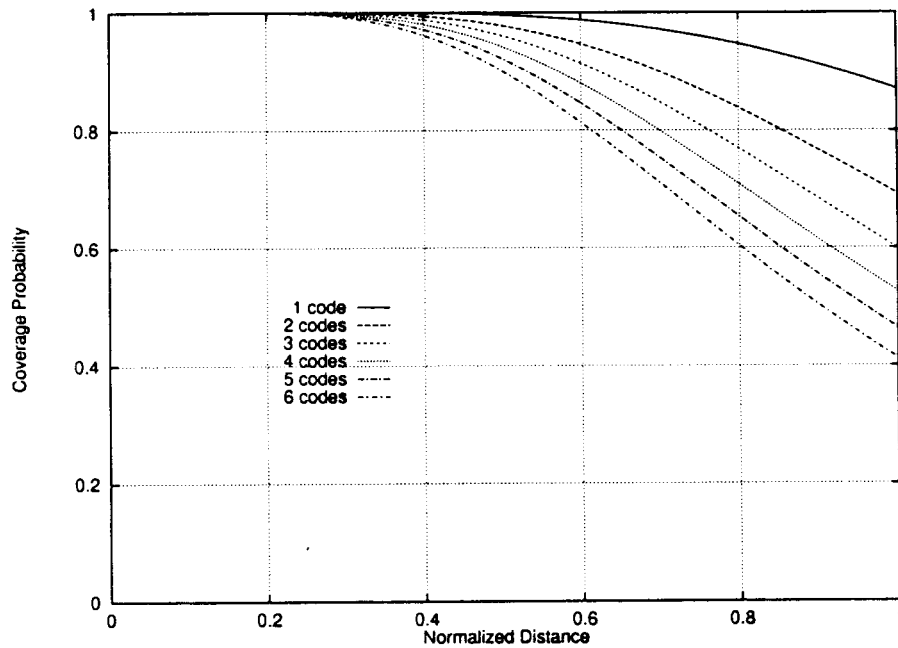
Fig. 12.   Reverse link coverage probability for type I mobile: 200-mW transmit power.

C. Mobile Transmit Power Budget

Let us examine the impact of higher data-rate transmissions on reverse link budget. In this section, we present coverage results for mobiles with various power limits. The reverse link budget is determined as follows. Given the maximum transmit power (P_T) of the mobile, we add to it all the gains (ΣG) (e.g., transmit and receive amplifier gains, transmit and receive antenna gains, spreading gain, and soft handoff gain), then we subtract all losses (ΣL) (e.g., connector and cable losses, fade margin, receiver noise figure, and the path loss to the edge of the cell). The result should be such that its ratio to the total noise plus interference power (I_0) meets the required E_b/N_0

$$P_T + \Sigma G - \Sigma L - I_0 = E_b/N_0 \text{ (dB)}. \qquad (19)$$

For a high data-rate mobile transmitting on m code channels, the transmit power per code channel (P_T) is reduced by 10 log m dB. There is an additional backoff due to the higher peak-to-average ratio of the total signal consisting of multiple code channels. This additional backoff is determined to vary from 2.0 and 4.0 dB as the number of code channels is increased from 2–8 [27]. Hence the coverage area over which the same E_b/N_0 is obtained reduces with increasing number of code channels. We assume that all the gain and loss factors including cell size in (19) are the same for voice and data mobiles, except for the transmit power per code channel. Then we can tradeoff the coverage area for number of code channels. We use a path loss exponent of four, shadow fading standard deviation of 8 dB, fade margin of 6 dB for voice, and a soft handoff gain of 3 dB [28].

Mobile Type I (200 mW) is data capable and has the same power amplifier and mobile form factor as today's voice-only mobiles, e.g., a personal digital assistant (PDA) with CDMA high data-rate capability. Type I mobiles at their power limit will be unable to burst at the highest rate until their fading and path loss condition improve. If the mobile is allocated a burst and receives many consecutive power-up commands when it is at its power limit, it can autonomously limit the number of codes on which to transmit. Thus it effectively reduces its data rate according to available power. Fig. 12 shows the coverage probability for a 200 mW mobile, transmitting at one to six times the basic rate, as a function of normalized distance from the BS.

Type II mobiles are special data mobiles that can attach to laptops and can use power amplifiers that are driven from the laptop battery. This effectively permits higher data rates to be achieved, using higher maximum transmit power. Fig. 13 shows the same results for a Type II mobile with 800 mW transmit power. Also, these mobiles may be able to exploit additional gain through the use of directional antennas, but that is not considered here.

Fig. 14 shows the mean number of codes that can be allocated as a function of distance for a 6× high data-rate mobile. We see that on average three codes can be provided even at the edge of the cell. Since bursts are allocated for short durations, this average is meaningful under user mobility.[5] Such averaging is not meaningful for circuit-mode data at high rate. Burst-mode coverage is provided over the entire coverage area. These curves show the available rate based on the mobile's power limit.

VIII.   REVERSE LINK POWER CONTROL

The static and dynamic capacity and coverage studies above assume perfect power control. It is well known that tight power

---

[5] This mean is over shadow fading. Individual locations within the coverage area may experience unacceptable coverage. A stationary mobile does not observe this averaging over shadow fading.
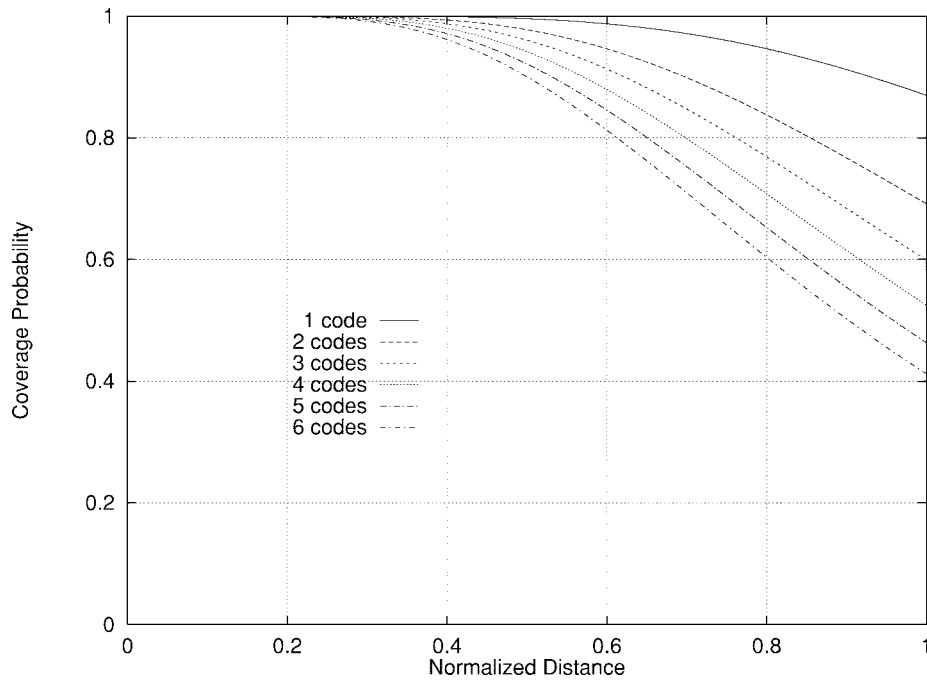
Fig. 13. Reverse link coverage probability for type II mobile: 800-mW transmit power.
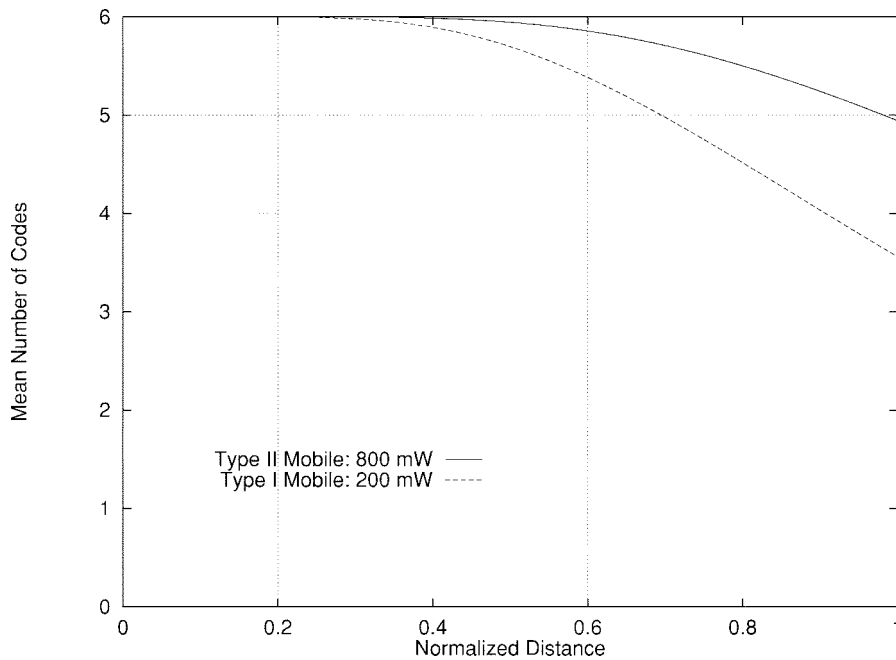

Fig. 14. Average number of codes permitted.

control is critical to CDMA capacity and performance. In this section we study reverse link closed-loop power control performance when the CDMA channel is shared between high data-rate users and voice. We report on several factors that permit reduction in the average E_b/N_0 requirement for high data-rate users. The smaller E_b/N_0 requirement translates to increased capacity (in terms of kb/s/cell/CDMA carrier).

The closed-loop power control is run on the the fundamental code channel since it is full duplex. The supplemental code channels are transmitted with the same power as the power-controlled fundamental.

A. Simulation Description

The simulation models the reverse link of a single cell or sector of an IS-95–based CDMA system. For simplicity, the out-of-cell interference is ignored. Therefore, the capacity results reported here must be scaled down by a factor f corresponding to a CDMA reuse factor [8]. In the cell under

consideration, we simulate a number of voice users that can be varied between one and N_v, a number of circuit-mode data users that can be varied between one and N_d, and one high data-rate user who simultaneously transmits on a number of code channels between one and M. The voice users follow a 16-state Markov voice activity model with a mean activity factor of 0.4. The circuit-mode data users are assumed to have an activity factor of one. The high data-rate user transmitting on multiple codes is assumed to also have an activity factor of one, as would be the case during a burst transmission. For simplicity, all users are assumed to be at the same velocity and have the same channel conditions. It is easy to extend the simulation to allow each user to have its own set of mobility and channel parameters, but it would be hard to obtain any great insight from this generalization while making the number of parameters to be managed prohibitive.

The simulation runs on a time step of 1.25 ms, the same as the power control inner loop step. In other work on power control performance, we have proposed and validated methods to model the physical layer performance while running the simulation at the coarser time scale. For details of this approach, the reader is referred to [29]. Based on this approach, the reverse link closed-loop power control is modeled in detail. An inner loop power control feedback bit is provided every 1.25 ms. As in IS-95 there is a two power control group delay in the feedback loop. The power control feedback bit error rate of 5% is fixed. The inner loop feedback is generated by comparing an estimate of the received E_b/N_0 with a set point determined by the outer loop power control that is designed to achieve a desired frame error rate target.

The channel is modeled as a Rayleigh fading, dispersive channel. The received signal at the BS consists of two or more multipath components received at the two receive antennas at the cell site. It is assumed that these multipath components can be resolved by the BS receiver which combines these signals weighted by the received energy in each path.

The results obtained from the simulation are in terms of the average E_b/N_0, defined as the the mean received signal level required to obtain a desired frame error rate, divided by the mean interference plus noise level at the receiver. The required E_b/N_0 depends not only on the signal variations, as determined by the user velocity and fading, number of multipaths, etc., but also the interference variations determined by the mix of voice, data, and high data-rate users sharing the channel within the cell. Independent power control loops are run for each voice, circuit-mode data, or high data-rate user. For the high data-rate user, all code channels undergo the same fading and follow the same power control. We find that correlated variation of the received power level of each supplemental code channel and the remaining code channels of the high data-rate user results in a reduction of the required E_b/N_0.

We also report the achieved FER and the mean rise over noise calculated as the ratio of the interference plus noise density at the given load to (no-load) noise density for a single cell. A smaller noise rise corresponds to the potential for higher capacity. The simulation results are for a carrier frequency of 900 MHz and a (default) power control step size

TABLE V
MULTIPLEXING OF N_v VOICE AND N_d CIRCUIT-MODE
DATA USERS (ALL USERS ARE AT 10 mi/h)

Voice Users N_v	Data Users N_d	Avg. E_b/N_0 (dB) Voice	Avg. E_b/N_0 (dB) Data	FER (%) Voice	FER (%) Data	Noise Rise (dB)
18	0	6.9	-	1.2	-	3.4
13	2	7.1	6.4	1.2	1.2	3.3
11	3	7.1	6.4	1.4	1.3	3.3
8	4	7.1	6.5	1.0	1.2	2.9
6	5	6.7	6.5	1.2	1.2	2.9
3	6	7.5	6.6	0.6	1.1	2.8
1	7	8.7	6.5	0.4	1.1	2.8
0	8	-	6.6	-	1.1	3.0

of 1 dB (unless otherwise stated). Simulations were run for 3000–10 000 frames.

B. E_b/N_0 Requirements

We find that data users with aggregated codes require a lower E_b/N_0 than data users with one code each. The E_b/N_0 requirement decreases with increase in code aggregation, i.e., the higher M, the number of codes per user, the lower the E_b/N_0 requirement. Tables VI and VIII show that the E_b/N_0 is reduced as M increases. At higher speeds, the required E_b/N_0 for 1% FER is larger, and correspondingly, the reduction in required E_b/N_0 due to code aggregation is also larger.

The reverse closed-loop power control adjusts according to the variations in interference seen from other users. In high-rate transmission, a significant part of the interference comes from other code channels transmitted by the user itself. That is, the interference seen from other codes channels of the high data-rate user is being powered controlled along with the desired signal. The variations in the interference correlate to the variations in the desired signal; therefore there is an E_b/N_0 advantage.

The increased variability of the interference seen by the voice users, when the bandwidth is shared with a high data-rate user, is reflected in the higher E_b/N_0 requirement for voice users.

C. Capacity Impacts

We next examine the capacity impact as a variable number of voice and data users are multiplexed on one CDMA carrier. For the same load (in terms of kb/s/sector/CDMA carrier), because of the E_b/N_0 advantage described above, the total noise rise is smaller when data users are present than when only voice users are present. The lower noise rise translates to an increase in capacity.

At both 1 and 10 mi/h, the total noise rise is smaller for the case of a single high data-rate user with M codes multiplexed with voice users (Tables VI and VIII), compared to the case of N_d circuit-mode data users multiplexed with voice users (Tables V and VII).

D. Smaller Power Control Step Size for Fixed Wireless Applications

The capacity for fixed wireless applications can be further increased through the use of a smaller power control step size. Table IX shows that the E_b/N_0 requirement can be decreased

TABLE VI
MULTIPLEXING OF N_v VOICE AND ONE HIGH DATA RATE
USER WITH M CODES (ALL USERS ARE AT 10 mi/h)

Voice Users N_v	Data Codes M	Avg. E_b/N_0 (dB) Voice	Avg. E_b/N_0 (dB) Data	FER (%) Voice	FER (%) Data	Noise Rise (dB)
18	0	6.9	-	1.2	-	3.4
13	2	6.6	6.4	1.4	1.2	2.9
11	3	6.9	5.9	1.4	1.3	3.0
8	4	6.6	6.0	1.4	1.1	2.5
6	5	6.9	5.9	1.5	1.2	2.5
3	6	8.1	5.7	0.8	1.0	2.4
1	7	8.0	5.6	0.8	1.1	2.1
0	8	-	5.4	-	1.2	2.1

TABLE VII
MULTIPLEXING OF N_v VOICE AND N_d CIRCUIT-MODE
DATA USERS (ALL USERS ARE AT 1 mi/h)

Voice Users N_v	Data Users N_d	Avg. E_b/N_0 (dB) Voice	Avg. E_b/N_0 (dB) Data	FER (%) Voice	FER (%) Data	Noise Rise (dB)
37	0	4.4	-	1.6	-	3.4
30	3	4.4	4.5	1.7	1.1	3.6
25	5	4.4	4.6	1.6	1.1	3.5
20	7	4.3	4.6	1.8	1.1	3.3
15	9	4.6	4.6	1.5	1.1	3.7
10	11	4.9	4.7	1.4	1.1	3.8
5	13	4.4	4.7	1.5	1.1	3.6
0	15	-	4.6	-	1.1	3.5

TABLE VIII
MULTIPLEXING OF N_v VOICE AND ONE HIGH DATA-RATE
USER WITH M CODES (ALL USERS ARE AT 1 mi/h)

Voice Users N_v	Data Codes M	Avg. E_b/N_0 (dB) Voice	Avg. E_b/N_0 (dB) Data	FER (%) Voice	FER (%) Data	Noise Rise (dB)
37	-	4.4	-	1.6	-	3.4
30	3	4.6	4.2	1.7	1.1	3.4
25	5	4.6	5.0	1.7	1.1	3.8
20	7	4.9	4.3	1.7	1.1	3.8
15	9	4.4	4.4	1.6	1.1	3.4
10	11	4.5	4.3	1.8	1.0	3.1
5	13	4.6	4.3	1.8	1.0	3.2
-	15	-	4.3	-	1.0	3.0

TABLE IX
MULTIPLEXING OF N_v VOICE AND ONE HIGH DATA-RATE USER WITH M
CODES (ALL USERS ARE AT 1 mi/h; POWER CONTROL STEP SIZE IS 0.5 dB)

Voice Users N_v	Data Codes M	Avg. E_b/N_0 (dB) Voice	Avg. E_b/N_0 (dB) Data	FER (%) Voice	FER (%) Data	Noise Rise (dB)
37	-	3.2	-	1.0	-	2.4
25	5	3.5	3.7	1.0	1.0	2.6
15	9	3.6	3.5	1.0	1.0	2.5
-	15	-	3.6	-	1.0	2.3

through the use of a step size of 0.5 dB instead of the current (default) value of 1.0 dB. The large step size is required for tracking performance in a rapidly fading mobile environment but is unnecessarily large for fixed wireless applications.

E. FER Target for Data Users

Unlike voice, the delay requirements for data permit the use of retransmissions over the noisy wireless link. This permits setting a higher FER target. In Table X we show the energy (capacity) gain from increasing the FER target to 4% from the current default value of 1% that is used for voice. The E_b/N_0 gain from increasing the FER target to 4% must be scaled

TABLE X
GAINS OBTAINED FROM INCREASING THE FER TARGET FOR DATA FROM 1–4%

Speed (mph)	Avg. E_b/N_0 (dB) at 1% FER	Avg. E_b/N_0 (dB) at 4% FER	Gain (dB)	Real Gain (dB)
1	4.4	3.7	0.7	0.6
10	6.6	5.0	1.6	1.5
15	7.7	5.8	1.9	1.8
20	8.2	6.3	1.9	1.8
30	8.2	6.0	2.2	2.1
60	7.2	5.3	1.9	1.8

back by 0.13 dB to account for the increase in the number of retransmitted frames. The real gain in E_b/N_0 is shown in the last column of Table X. The gains are over 1.5 dB at speeds higher than 10 mi/h.

F. Summary

We have found several factors that permit reduction in the average E_b/N_0 requirement for high data-rate users. In particular, items 1) and 2) below apply to the case of high data-rate user using multiple code channels on the reverse link. Items 3)–5) are equally applicable to the case of multiple code channels or variable spreading gain, as in the third-generation proposals. The smaller E_b/N_0 requirement translates to increased capacity (in terms of kb/s/cell/CDMA carrier). Our findings are as follows.

1) High data-rate users have a lower E_b/N_0 requirement compared to voice users or circuit-mode data users.
2) Voice users see a small increase in E_b/N_0 requirement when sharing a CDMA carrier with high data-rate users. However, there is an overall capacity gain as reflected in a smaller noise rise.
3) The E_b/N_0 requirements are smaller by almost 2 dB at 1 mi/h compared to 30 mi/h. This implies a larger capacity if high data-rate mobiles are stationary or fixed wireless users.
4) There is a further decrease in E_b/N_0 requirement (almost 1 dB) and gain in capacity by decreasing the power control step size to 0.5 dB.
5) Finally, there is a further gain of over 0.6 dB in E_b/N_0 requirement by setting a higher FER target for delay-tolerant data services allowing for recovery through retransmissions.

As a result of all these factors, we conclude that there is actually a large increase in the reverse link capacity (in terms of kb/s/cell/CDMA carrier) when high data-rate users are introduced. The simulations also dispel the predicted adverse performance impacts of code aggregation.

IX. CONCLUSIONS

We have proposed a solution to provide packet services over cellular systems based on CDMA. Wideband CDMA systems are being proposed and standardized for third-generation cellular systems around the world. Our proposed LIDA resource allocation scheme is applicable to both current and future systems. New messages and procedures that permit such burst-

mode operation have already been standardized in Revision B of the IS-95 CDMA cellular standard [22].

We studied capacity and coverage performance of our scheme. Simple static analysis and Monte Carlo simulations were used to determine the feasibility of the scheme. Having established that the scheme is worth pursuing, we proposed a dynamic simulation to study the performance of the burst-allocation schemes.

Using the dynamic simulation approach and analytic calculation of interference through superposition, we determined results for reverse link capacity when the CDMA carrier is shared between voice and burst-mode high-speed packet data users. For the forward link, we used the dynamic simulation to study the performance of forward burst allocation on a subset of legs in soft handoff. The capacity advantage of this burst allocation on fewer legs is traded off with FER performance on the supplementals.

We also examined the impact of nonideal power control on reverse link capacity. We found several factors that result in higher capacity than in the voice-only system.

Observations related to the performance analysis are included in the related section. Our studies demonstrate the feasibility of packet services over CDMA and wideband CDMA. In this paper we have addressed several important issues in some depth. However, we expect that this is just the beginning, and much additional performance work will become available as higher data-rate services over cellular and third-generation wideband CDMA system become widespread around the world.

APPENDIX
OUT-OF-CELL INTERFERENCE CALCULATIONS

Consider the three cells I, II, and III, shown in Fig. 15. Each is sectorized into three sectors, α, β, and γ. We assume that mobiles are uniformly distributed, N_v per sector. Here we do not consider the speech activity factor. The reduction in interference because of the speech activity factor of the interfering mobiles is accounted for separately. We compute the average interference seen at the cell site I sector γ due to the mobiles in cells II and III. Since cells II and III are identical, we need only consider one of them.

To compute the interference from sector α of cell II, we further subdivide the sector into two equilateral triangles denoted $T2$ and $T4$ in the figure. As in Gilhousen *et al.* [8], for a random mobile in $T2$ at (x, θ), at a distance y from cell site I, assuming that the mobile is perfectly power controlled to compensate for the distance loss and shadow fading to cell site II, the interference to signal ratio at cell site I sector γ may be written as

$$\frac{I}{S}(x, y, \xi_{\mathrm{I}}, \xi_{\mathrm{II}}) = \left[\frac{10^{\xi_{\mathrm{II}}/10}}{y^4}\right]\left[\frac{x^4}{10^{\xi_{\mathrm{I}}/10}}\right]$$

$$= \left[\frac{x}{y}\right]^4 10^{(\xi_{\mathrm{II}}-\xi_{\mathrm{I}})/10}$$

$$= \left[\frac{x}{y}\right]^4 10^{\xi/10}$$

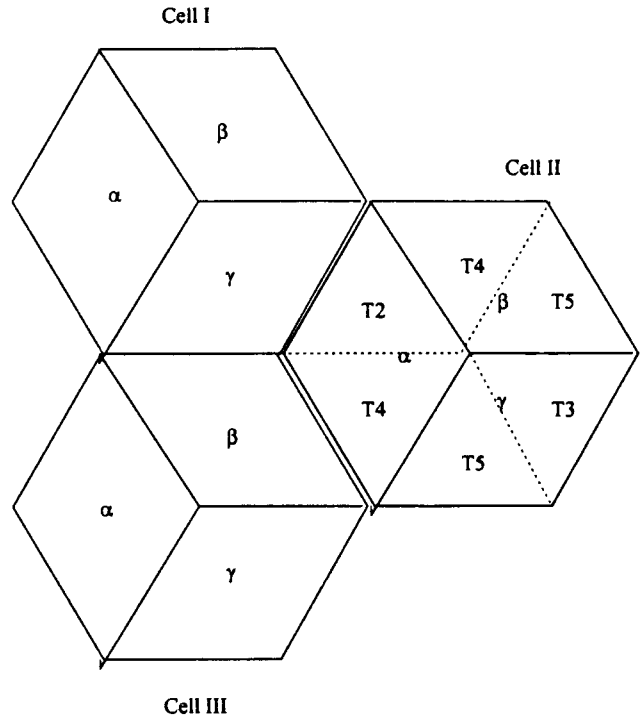$$= \frac{I}{S}(x, y, \xi) \leq 1 \qquad (20)$$

Fig. 15. Two neighbor cells used for out-of-cell interference calculation.

where ξ_{I} and ξ_{II} are the exponents of the shadow fading in cells I and II, i.e., normal with variance σ^2. ξ is normal with standard deviation $2\sigma^2$. We make the following "soft handoff" assumption: $I/S \leq 1$; the mobile is an interferer at cell site I only if it is connected to the other cell site, that is, its path loss (distance loss and shadow fading) to cell site II is smaller.

We compute the mean I/S from mobiles uniformly distributed in the $T2$. Since the representative mobile position is uniformly distributed in sector α of cell site II. The pdf is $\rho = 1/A_\alpha$, where $A_\alpha = \sqrt{3}/2$ is the area of the sector

$$E[I/S]_{T2} = \iint_{T2} \left[\frac{x}{y}\right]^4 E\left[10^{\xi/10}I_{(I/S)\leq 1}\right]\frac{dA}{A_\alpha}. \qquad (21)$$

The expectation, in the integrand, over ξ with a normal kernel with variance $2\sigma^2$ can be computed as a function of x, y and σ, the parameters of the indicator function $I_{(I/S)\leq 1}$ in (21). In the Appendix of [8] this expectation is shown to be

$$f\left(\frac{x}{y}\right) = E\left[10^{\xi/10}I_{(I/S)\leq 1}\right]$$

$$= e^{(\sigma \ln 10/10)^2}\left\{1 - Q\left[\frac{40\log(y/x)}{\sqrt{\sigma^2}} - \sqrt{\sigma^2}\frac{\ln 10}{10}\right]\right\}. \qquad (22)$$

Note that by setting $f(\ )$ identically to one, the computation reduces to one without shadow fading. We denote the interference factor from Tn as $i_{Tn} = E[I/S]_{Tn}$, which is the interference per uniformly distributed user in Tn. The integrals for Tn have been computed using numerical integration in Mathematica. We have used a shadow fading standard deviation of 6.8 dB. The results are tabulated in Table XI.

TABLE XI
FER Target for Data Users

Interference Factors	Lognormal Fading (6.8 dB std. dev.)	No Lognormal Fading, $f() = 1$
i_{T2}	0.0562	0.1141
i_{T3}	0.0043	0.0016
i_{T4}	0.0424	0.0315
i_{T5}	0.0228	0.0053

The interference factors for the three sectors are computed as follows:

$$i_{\alpha} = i_{T2} + i_{T4}$$
$$i_{\beta} = i_{T4} + i_{T5}$$
$$i_{\gamma} = i_{T3} + i_{T5}.$$

Again, note that these interference factors are for cell site II. The interference factors from cell site III are identical. Also, the interference reduction due to speech activity is not included in these interference factors.

ACKNOWLEDGMENT

REFERENCES

[1] E. Ayanoglu, K. Y Eng, and M. J. Karol, "Wireless ATM: Limits, challenges and proposals," *IEEE Personal Commun. Mag.*, vol. 3, pp. 18–34, Aug. 1996.

[2] *IEEE Personal Commun. Mag.*, "Special Issue on Wireless ATM," vol. 3, Aug. 1996.

[3] S. Nanda, D. J. Goodman, and U. Timor, "Performance of PRMA: A packet voice protocol for cellular networks," *IEEE Trans. Veh. Technol.*, vol. 40, pp. 584–598, Aug. 1991.

[4] B. Tuch, "WaveLAN, an ISM band wireless LAN," *AT&T Tech. J.*, vol. 72, no. 4, pp. 27–37, Aug. 1993.

[5] M. Karol, Z. Liu, and K. Y. Eng, "An efficient demand-assignment multiple access protocol for wireless packet (ATM) networks," *ACM/Baltzer Wireless Networks*, vol. 1, no. 2, pp. 161–174, 1995.

[6] J. F. Whitehead, "Distributed packet dynamic resource allocation (DRA) for wireless networks," in *Proc. 46th IEEE Vehicular Technology Conf.*, 1996, pp. 111–115.

[7] J. C. Chuang and N. R. Sollenberger, "Medium access control for advanced cellular internet services," in *Proc. 8th IEEE Int. Symp. Personal, Indoor and Mobile Radio Communications*, 1997, pp. 673–677.

[8] K. S. Gilhousen, I. M. Jacobs, R. Padovani, A. J. Viterbi, L. A. Weaver, and C. E. Wheatley III, "On the capacity of a cellular CDMA system," *IEEE Trans. Veh. Technol.*, vol. 40, pp. 303–312, May 1991.

[9] A. J. Viterbi, A. M. Viterbi, and E. Zehavi, "Other-cell interference in cellular power controlled systems," *IEEE Trans. Commun.*, vol. 42, pp. 1501–1504, Feb./Apr. 1994.

[10] N. D. Wilson, R. Ganesh, K. Joseph, and D. Raychaudhuri, "Packet CDMA versus dynamic TDMA for multiple access in an integrated voice/data PCN," *IEEE J. Select. Areas Commun.*, vol. 11, pp. 870–884, Aug. 1993.

[11] D. N. Knisely, S. Kumar, S. Laha, and S. Nanda, "Evolution of wireless data services: IS-95 to cdma2000," *IEEE Commun. Mag.*, vol. 36, pp. 140–149, Oct. 1998.

[12] S. Kumar and S. Nanda, "An access scheme for high speed packet data service on IS-95 based CDMA," in *WINLAB Workshop 1997, Proc. Advances in Wireless Communications*, 1998, pp. 241–252.

[13] S. Kumar, S. Nanda, and A. Falconi, "Reverse link power control performance for high speed data over CDMA," in *Proc. Int. Conf. Telecommunications 1998*, Porto Carras, Greece, pp. 403–407.

[14] S. Kumar and S. Nanda, "A simulation technique to study CDMA system performance with integrated voice and data services," in *Proc. Applied Telecommunications Symp. 1998*, Boston, MA, pp. 86–91.

[15] C.-L. I and S. Nanda, "Load and interference based demand assignment for wireless CDMA networks," in *Proc. IEEE Globecom*, 1996, pp. 235–241.

[16] _____, "Cellular interference control for integrated services over CDMA," in *Proc. International Teletraffic Congr.*, Washington, DC, June 1997, pp. 1–11.

[17] M. Gudmundson, "Correlation model for shadow fading in mobile radio systems," *Electron. Lett.*, vol. 27, no. 23, pp. 2145–2146, 1991.

[18] A. Mawira, "Models for the spatial correlation functions of the (log)-normal component of the variability of VHF/UHF field strength in urban environment," in *3rd IEEE Int. Conf. Personal, Indoor and Mobile Radio Communications*, 1992, pp. 436–440.

[19] N. B. Mandayam, P. Chen, and J. M. Holtzman, "Minimum duration outage for cellular systems: A level crossing analysis," *IEEE Vehicular Technology Conf.*, 1996, pp. 879–883.

[20] R. P. Ejzak, D. N. Knisely, S. Kumar, S. Laha, and S. Nanda, "BALI: A solution for high-speed CDMA data," *Bell Labs Tech. J.*, vol. 2, no. 3, pp. 124–151, Summer 1997.

[21] Telecommunications Industry Association (TIA), *EIA/TIA-95 Rev A: Mobile Station-Base Station Compatibility Standard for Dual-Mode Wideband Spread Spectrum Cellular System*, 1995.

[22] _____, *EIA/TIA-95 Rev B: Mobile Station-Base Station Compatibility Standard for Dual-Mode Wideband Spread Spectrum Cellular System*, Oct. 1998.

[23] _____, *IS-99: Data Services Option Standard for Wideband Spread Spectrum Cellular System*, July 1995.

[24] _____, *IS-657: Packet Data Services Standard for Wideband Spread Spectrum Digital Cellular System*, July 1996.

[25] _____, *IS-707: Data Services Standard for Wideband Spread Spectrum Cellular System*, Nov. 1998.

[26] C.-L. I, C. Webb, H. Huang, S. Ten Brink, S. Nanda, and R. Gitlin, "IS-95 enhancements for multimedia services," *Bell Labs Tech. J.*, vol. 1, no. 2, pp. 60–87, Autumn 1996.

[27] L. Mailaender, private communication, Sept. 1997.

[28] A. J. Viterbi, *CDMA: Principles of Spread Spectrum Communication*. Reading, MA: Addison-Wesley, 1995.

[29] S. Nanda and K. Rege, "Frame error rates for convolutional codes on fading channels and the concept of effective E_b/N_0." in *Proc. Globecom 1995 Communication Theory Mini Conf.*, pp. 27–32.

[30] _____, "Error performance of convolutional codes in fading environments: Heuristics for effective E_b/N_0 computation," in *Proc. Conf. Information Sciences and Systems (CISS)*, Princeton, NJ, Mar. 1996.
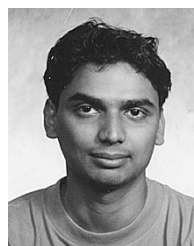
Sarath Kumar received the B.Tech. degree in electrical engineering from the Indian Institute of Technology, Kanpur, in 1988, the M.Tech. degree from the Indian Institute of Technology, Bombay, in 1990, and the Ph.D. degree in electrical engineering from the University of Pennsylvania, Philadelphia, in 1993. For his Ph.D. dissertation, he worked on multi-user transmitter/receiver design.

From October 1993 to April 1994, he worked as a Research Associate at the Wireless Information Networks Laboratory (WINLAB), Rutgers University, Piscataway, NJ. At WINLAB, he looked at the resource allocation issues in cellular communications. Since May 1994, he has been with the Performance Analysis Department at Bell Laboratories, Lucent Technologies, Holmdel, NJ. He is currently involved in the design and analysis of CDMA networks.
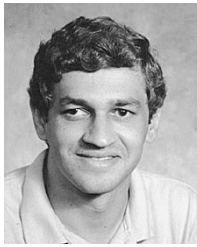
Sanjiv Nanda (S'85–M'88) received the B.Tech. degree in electrical engineering from the Indian Institute of Technology, Kanpur, in 1983 and the M.S. degree in mathematics in 1986 and the M.S. and Ph.D. degrees in electrical engineering in 1985 and 1988, respectively, all from the Rensselaer Polytechnic Institute, Troy, NY.

During 1989–1990, he was with the Wireless Information Network Laboratory (WINLAB), Rutgers University, Piscataway, NJ. Since 1990, he has been with the Performance Analysis Department at Bell Labs, Lucent Technologies, Holmdel, NJ, where he is currently Technical Manager. At Lucent, he has worked on many aspects of cellular system design, including system architecture, protocol design, system performance, and link performance. He has made contributions to Lucent's wireless products through algorithms, performance analysis, and participation in standards and architecture teams. He has published several papers and holds eight U.S. patents.

Dr. Nanda co-authored a paper on AAL-2 that was chosen as the Best Paper in Networking in the *Bell Labs Technical Journal* in 1997. His paper on PRMA with Goodman and Timor won the IEEE Vehicular Technology Society's Jack Neubauer Award for the best systems paper published in the IEEE TRANSACTIONS ON VEHICULAR TECHNOLOGY in 1991.